

Humanization of JAA-F11, a Highly Specific Anti-Thomsen-Friedenreich Pancarcinoma Antibody and *In Vitro* Efficacy Analysis



Swetha Tati^{†,1}, John C. Fisk^{†,1}, Julia Abdullah^{*,†,‡}, Loukia Karacosta[†], Taylor Chrisikos^{*,†}, Padraic Philbin^{*}, Susan Morey^{*}, Diala Ghazal[†], Fatma Zazala[†], Joseph Jessee[†], Sally Quataert[†], Stephen Koury^{*}, David Moreno^{*}, Jing Ying Eng^{*}, Vladislav V. Glinsky^{§,¶}, Olga V. Glinskii^{§,#}, Muctarr Sesay^{**}, Anthony W. Gebhard^{**}, Karamveer Birthare^{**}, James R. Olson^{†,††} and Kate Rittenhouse-Olson^{*,†}

*Department of Biotechnical and Clinical Laboratory Sciences, University at Buffalo, Buffalo, NY; [†]For-Robin, Inc., Buffalo, NY; [‡]Department of Microbiology and Immunology, University at Buffalo, Buffalo, NY; [§]Research Service, Harry S. Truman Memorial Veterans Hospital, Columbia, MO; [¶]Department of Pathology and Anatomical Sciences, University of Missouri, Columbia, MO; [#]Department of Medical Pharmacology and Physiology, University of Missouri, Columbia, MO; ^{**}Goodwin Biotechnology, Inc., Plantation, FL; ^{††}Department of Pharmacology and Toxicology, University at Buffalo, Buffalo, NY

Abstract

JAA-F11 is a highly specific mouse monoclonal to the Thomsen-Friedenreich Antigen (TF-Ag) which is an alpha-O-linked disaccharide antigen on the surface of ~80% of human carcinomas, including breast, lung, colon, bladder, ovarian, and prostate cancers, and is cryptic on normal cells. JAA-F11 has potential, when humanized, for cancer immunotherapy for multiple cancer types. Humanization of JAA-F11, was performed utilizing complementarity determining regions grafting on a homology framework. The objective herein is to test the specificity, affinity and biology efficacy of the humanized JAA-F11 (hJAA-F11). Using a 609 target glycan array, 2 hJAA-F11 constructs were shown to have excellent chemical specificity, binding only to TF-Ag alpha-linked structures and not to TF-Ag beta-linked structures. The relative affinity of these hJAA-F11 constructs for TF-Ag was improved over the mouse antibody, while T20 scoring predicted low clinical immunogenicity. The hJAA-F11 constructs produced antibody-dependent cellular cytotoxicity in breast and lung tumor lines shown to express TF-Ag by flow cytometry. Internalization of hJAA-F11 into cancer cells was also shown using a surface binding ELISA and confirmed by immunofluorescence microscopy. Both the naked hJAA-F11 and a maytansine-conjugated antibody (hJAA-F11-DM1) suppressed *in vivo* tumor progression in a human breast cancer xenograft model

Abbreviations: Ab, Antibodies; ADCC, Antibody-dependent cellular cytotoxicity; Ag, Antigen; BLAST, Basic local alignment search tool; BSA, Bovine serum albumin; CDC, Complement-dependent cytotoxicity; CDRs, Complementarity determining regions; CHO, Chinese hamster ovary; CMV, Cytomegalovirus; DNA, Deoxyribonucleic acid; *E. coli*, *Escherichia coli*; EIA, Enzyme immunoassay; ELISA, Enzyme-linked immunosorbent assay; FCS, Fetal calf serum; FRs, Framework regions; Gal, Galactose; GalNAc, N-acetyl galactosamine; GlcNAc, N-acetyl glucosamine; HC, Heavy chain; Ig, Immunoglobulin; IgG, Immunoglobulin G; IgG1, Immunoglobulin G class 1; LC, Light chain; LDH, Lactate dehydrogenase; mAb, monoclonal antibody; NeuAc, Sialic acid; OD, Optical density; PBS, Phosphate buffered saline; PCR, Polymerase chain reaction; RNA, Ribonucleic acid; SD, Standard deviation; SEM, Standard error of the means; TF-Ag, Thomsen-

Friedenreich antigen; VH, Variable region heavy chain; VL, Variable region light chain.

Address all correspondence to: Kate Rittenhouse-Olson, Department of Biotechnical and Clinical Laboratory Sciences, University at Buffalo, Buffalo, NY.

E-mail: krolson@buffalo.edu

¹ Dual first author.

Received 25 May 2017; Revised 19 July 2017; Accepted 24 July 2017

© 2017 The Authors. Published by Elsevier Inc. on behalf of Neoplasia Press, Inc. This is an open access article under the CC BY-NC-ND license (<http://creativecommons.org/licenses/by-nc-nd/4.0/>).

1476-5586

<http://dx.doi.org/10.1016/j.neo.2017.07.001>

in SCID mice. Together, our results support the conclusion that the humanized antibody to the TF-Ag has potential as an adjunct therapy, either directly or as part of an antibody drug conjugate, to treat breast cancer, including triple negative breast cancer which currently has no targeted therapy, as well as lung cancer.

Neoplasia (2017) 19, 716–733

Background

Thomsen-Friedenreich antigen (TF-Ag) is a carbohydrate pancarcinoma antigen expressed on ~80% of human carcinomas including breast, lung, colon, bladder, ovary, prostate and stomach cancers, [1–10] but is cryptic on normal tissues. TF-Ag is also found on leukemia and lymphoma cells [11,12]. TF-Ag is expressed on tumor tissues due to changes in glycosylation in tumor cells which increases the expression of core saccharide structures devoid of further glycosylation, as opposed to normal cells where TF-Ag is hidden due to the addition of carbohydrate moieties [13–15]. TF-Ag is the disaccharide D-galactose-beta-(1–3)-N-acetyl galactosamine (Gal- β -(1–3)-GalNAc) which is alpha linked to a serine or a threonine residue on proteins [1]. The same disaccharide structure can appear beta-linked on glycolipids in normal tissues, so this linkage inclusion is important for tumor specificity [13]. Thus, the tumor restricted presence of this antigen makes this a promising target for cancer immunotherapy. In addition, TF-Ag plays a pivotal role in metastasis [16–22] where tumor cell surface TF-Ag binds and causes up-regulation of Galectin-3 (Gal-3) expression and mobilization on the surface of vascular endothelial cells. The TF-Ag and Gal-3 binding interaction causes the arrest of the tumor cell on the blood vessels followed by the endothelial integrin $\alpha 3\beta 1$ stabilization/locking event, all steps required for establishing metastasis [23]. Further evidence supporting the role of TF-Ag in tumor metastasis stems from clinical studies showing that tumors that have greater metastatic activity were found to over-express TF-Ag [3–5,10]. Therefore, we hypothesized that therapy with an anti-TF antibody could create a survival advantage for patients with TF-Ag expressing tumors through direct killing, antibody-linked drug conjugate killing and/or by blocking tumor cell spread.

The murine monoclonal IgG₃ antibody JAA-F11 [24] is highly specific in that it binds to the alpha-linked tumor-associated TF-Ag and not the beta-linked structure known to be localized on the surface of normal tissues such as the kidney and natural killer (NK) cells [25–27]. The *in vivo* specificity of JAA-F11 was observed using iodine 124-labeled JAA-F11 in the mouse 4T1 breast cancer model, the nude-xenograft human breast cancer model (MDA-MB-231(triple negative)) and the SCID-xenograft human breast cancer model (with DU4475 triple negative tumors) [27–29]. Notably, JAA-F11 did not significantly bind to the kidneys or other organs in the mice, which is a promising indicator of safety and specificity for future therapy and diagnostic imaging in humans. Conversely, the less specific anti-TF-Ag murine antibody, Tru-Scint MAb 170H.82, which appears to bind to both the alpha- and beta-linked TF-Ag, was withdrawn after Phase III clinical trials, possibly because despite the promising tumor imaging sensitivity observed, this antibody also bound normal kidney tissue [29]. Studies have shown that JAA-F11 blocks metastasis in an established *in vivo* 4T1 metastatic breast cancer model, as well as in *in vitro* and *ex vivo* models [16]. Previous *in vitro* whole cell binding assays revealed that JAA-F11 targets approximately 80% of 41 breast cancer cell lines tested, regardless of estrogen receptor (ER), progesterone receptor (PR) or Her2 status,

targeting ability that included 82% of triple negative breast cancers tested (TNBC) [28]. Furthermore, we recently demonstrated that JAA-F11 is rapidly internalized by tumor cells within 1 hour [28]. This property can be exploited to bring drugs or toxins into the cancer cells in a more targeted way to reduce normal cell toxicity and increase tumor cell killing [30,31]. Altogether, these pre-clinical data obtained with JAA-F11 suggest this antibody as a potential therapeutic agent for the treatment of cancer.

The fact that TF-Ag is associated with many human cancers, including triple negative breast cancer, warrants its exploitation for therapeutic uses. Murine antibodies, however, have limited therapeutic applications due to their immunogenicity, short serum half-lives, and weak human effector functions [32–34]. Human immune response to mouse JAA-F11 prevents its direct clinical use, so humanization is necessary to decrease the immunogenicity of the mouse antibody and to allow it to remain in circulation for a longer time. As humanization can affect specificity and affinity because the framework regions can have an effect on conformation, understanding and conserving the initial antibody structure and testing the humanized constructs is important. This specificity is particularly important in our anti-carbohydrate antibody response since TF-Ag alpha is tumor associated while TF-Ag beta is on normal tissues.

Here we report the construction, production, and characterization of two humanized variants of the mouse mAb JAA-F11. Humanization of JAA-F11 was achieved by using a complementarity determining region (CDR) grafting process for the mouse VL and VH regions and subsequent construction into a full length human IgG1 antibody. The antibody was produced in CHO-K1 cells after stable transfection with two recombinant expression vectors. The purified hJAA-F11 antibodies were compared to the mouse [13,16,18,23,24,27,28,37] and chimeric JAA-F11 in terms of specificity, relative affinity, and effector functions. The overall goal of this study is to generate a humanized monoclonal antibody to the tumor antigen TF-Ag, which has high specificity, low immunogenicity and high biological efficacy.

Materials and Methods

Human use Ethics Statement

Blood for cytotoxicity assays was obtained voluntarily from healthy donors with approval (421397–4) granted by University at Buffalo Health Science Institutional Review Board.

Cells, Cell Lines, and Mammalian Expression Vectors

Adherent Chinese hamster ovary cells (CHO-K1; ATCC #CCL-61™, Manassas, VA) were maintained in Ham's F12 medium (Corning Cellgro, Manassas, VA) supplemented with 10% fetal calf serum (FCS; Hyclone) at 37°C and 5% carbon dioxide (CO₂) in humidified air. The tumorigenic human breast cancer cell line MDA-MB-231 was kindly provided by Dr. Julian Gomez-Cambronero (Wright State University,

Ohio). The mouse breast cancer cell line 4T1 was obtained from Fred Miller (University of Michigan). The breast cancer cell lines MDA-Kb2, SKBR-3, MDA-MB-453, MDA-MB-468, DU4475, HCC-1806 and BT549 were obtained from the American Type Culture Collection (ATCC breast cancer panel ATCC #30-4500K™, ATCC, Manassas, VA) and maintained in recommended media. Lung cancer cell lines NCI-H446 (ATCC #HTB-171™), A549 (ATCC #CRM-CCL-185™), NCI-H520 (ATCC #HTB-182™) and NCI-H460 (ATCC #HTB-177™) were obtained from the American Type Culture Collection (ATCC, Manassas, VA) and maintained in recommended media. Peripheral blood mononuclear cells (PBMCs) for antibody-dependent cellular cytotoxicity (ADCC) assays were isolated from whole blood obtained from healthy donors by density gradient centrifugation using Ficoll-Paque Plus (GE Healthcare) according to manufacturer's instructions (SUNY University at Buffalo Health Sciences IRB (HSIRB) Project: 421,397–4).

Two mammalian expression vectors, 6307 pAH and 6714 pAN, were kindly provided by Dr. Sherie L. Morrison (University of California, Los Angeles). The 6307 pAH vector contains the human IgG1 heavy chain leader/constant region under the control of human cytomegalovirus (CMV) promoter, and has an ampicillin (Amp) and histidinol dehydrogenase (*hisD*) gene cassettes for selection; while the 6714 pAN vector carries a human kappa light chain leader/constant region under the control of the human CMV promoter and has a neomycin phosphotransferase (*neoR*) cassette for selection. Two other mammalian expression vectors were also obtained from InvivoGen (San Diego, CA) for expression of human IgG1 heavy chains (pFUSE-ChIg-hIg1) and human kappa light chains (pFUSE2-CLIg-hK) which express resistance to zeomycin and blasticidin respectively.

Cloning and Sequencing of JAA-F11 Antibody Variable Regions

Cloning and sequencing of variable heavy (VH) and light (VL) genes of murine JAA-F11 mAb were performed after isolation of total RNA from JAA-F11 hybridoma cells using an RNeasy mini isolation kit (Qiagen, Louisville, KY) according to the manufacturer's instructions. First strand cDNA was synthesized via the Reverse Transcription System (Promega, Madison, WI) using oligo (dT) primers. Amplification of the VL gene was performed using mixture of six leader region primers and a mixture of three J region primers [35]. The VH gene was amplified using gene specific primers: 5'-TCTGGGGCTGAAGCTGGCAAAA-3' (forward primer) and 5'-CTTGGGTATTCTAGGCTCGATTCTC-3' (reverse primer). All primers were synthesized by Invitrogen, Grand Island, NY. The PCR products were ligated into a pGEM-T Easy cloning vector (Promega, Madison, WI) for sequencing analyses.

Humanization of JAA-F11

The CDRs were optimized using the Kabat [36] and Chothia [37] numbering systems, as well as crystal structure, glycan array and computational carbohydrate threading data [38]. Thus the CDRs also included mouse JAA-F11 framework residues located 5–6 angstroms (Å) from the antigen binding site obtained from the crystallography and computational carbohydrate threading data described in Tessier et al. [38], as well as two cysteines at positions L23 and L88 of the light variable chain, which are involved in disulfide bonds. To select the most mouse-like human germline sequence the IGMT database was searched (<http://www.imgt.org/>) by removing the mouse CDRs from the sequence, and blasting the database for the most similar human germline sequence FR.

To choose an alternate human acceptor antibody FR, two separate Protein BLAST® (BLASTP) searches against the entire non-redundant human (*Homo sapiens*) Genbank database were performed for the heavy and light chain variable regions of mouse JAA-F11. All non-*Homo sapiens* protein sequences, humanized antibodies and phage display sequences were eliminated from the BLASTP results. The resulting top 10 most homologous sequences of each of the heavy and light chain variable sequence of JAA-F11 were selected for the development of the human acceptor antibody framework for the humanized JAA-F11 (hJAA-F11). At each spot in the framework of both the heavy and light variable region sequence the most frequently occurring human amino acid among these top 10 selected human FR sequences was chosen to replace the framework mouse amino acid except the 3 amino acids on either side of the CDR were kept as mouse. These proposed hJAA-F11 constructs were assessed for conformational effects on the binding site in collaboration with Dr. Andrew Gulick at the Hauptmann Woodward Institute. The heavy chains had a proposed replacement for alanine using arginine at position 72 that could potentially cause significant steric interaction with surrounding amino acids. Similarly, a leucine at position 51 for the light chain was replaced with arginine which could result in steric clashes with surrounding amino acids side chains. These conflicting substitutions were removed and replaced with the original mouse JAA-F11 framework residue, alanine 72 (VH) and leucine 51 (VL). A chimeric JAA-F11 was also constructed in which the entire mouse JAA-F11 variable region was attached to a human IgG1 constant region. This provided a baseline that should have the original specificity and affinity of the mouse antibody while having the human constant region, to be used as a control for evaluating the humanized variant.

Construction of Humanized and Chimeric Antibody Expression Vectors

The gene coding sequences for VH and VL chain variable regions of humanized and chimeric JAA-F11 were synthesized (Genscript, Piscataway, NJ) with the inclusion of appropriate restriction enzyme sites, and cloned into the pUC57 vector. To construct the humanized and chimeric heavy chain expression vectors, cloned humanized JAA-F11 and chimeric heavy chain variable region DNA (VH) each were excised from the pUC57 vector and ligated into the 6307 pAH vector generating the humanized and chimeric heavy chain expression vectors. The humanized and chimeric light chain vectors were obtained by excising the cloned humanized JAA-F11 and chimeric heavy chain variable region DNA (VH) each from pUC57 vector and inserting into the 6714 pAN vector. Before transfecting into mammalian cells, all expression vectors were verified by DNA sequencing. A similar strategy was also used to clone into the heavy chain vector pFUSE-ChIg-hG1 and the light chain vector pFUSE2-CLIg-hK.

Immunogenicity Prediction

To determine the immunogenicity of the proposed humanized JAA-F11 variable region, a prediction was performed using the T20 scoring method which was developed by Gao et al. [39] to calculate the “humanness” of monoclonal antibody variable region sequences. A blast of the variable region was performed against the T20 Cutoff Human Database available online at <http://abanalyzer.lakepharma.com/>. The humanized antibody variable region was compared to the top 20 human Ab BLAST matches and scored for similarity to these sequences. The T20 score for humanized antibody is obtained from the average of the percent identities of the top 20 matched human sequences. To be considered not immunogenic, T20 scores of the FR and CDR

sequences must be above 80, and T20 scores for the FR sequences only must be above 85. Scores near or above these values are predicted to be of low immunogenicity [39].

Stable Expression and Production of Humanized and Chimeric Antibodies

For stable transfection into mammalian cells, an endotoxin-free plasmid isolation of humanized or chimeric heavy and light chain expression vectors was performed using PureYield Plasmid Midiprep System (Promega, Madison, Wisconsin) according to manufacturer's instructions. Linearization was performed using the PvuI restriction enzyme (Promega, Madison, WI), and extracted using the S&S Elutrap electro-separation system (Schleicher & Schuell, Dassel, Germany) as per manufacturer's instructions. Five micrograms of each linearized heavy and light chain vector were added to 5×10^6 CHO-K1 cells in cold Ham's F12 medium in a total volume of 500 μ L in a 0.4 cm electroporation cuvette (Bio-Rad, Hercules, CA). Following electroporation (Bio-Rad Gene Pulser, 960 μ F and 250 mV), the cells were diluted with pre-warmed non-selective medium (Ham's F12 supplemented with 10% FCS) to 1×10^5 cells/mL and plated into 96-well flat bottom tissue culture plates (BD Bioscience, San Jose, CA) at a density of 1×10^4 cells per well (200 μ L/well). The transfected cells were incubated at 37°C and 5% CO₂. Stable transfectants were selected with 700 μ g/mL G418 (Geneticin) and 5 mM of Histidinol by limiting dilution. The culture supernatants were analyzed by enzyme-linked immunoassay (ELISA) for antibody production using TF-Ag coated plates as previously described [16]. The clones producing the highest amount of humanized or chimeric JAA-F11 were selected and expanded. The humanized and chimeric antibodies were purified using a Protein A-Sepharose[®] 4B, Fast Flow affinity column (Sigma-Aldrich, St Louis, MO). For continuous production of hJAA-F11, the best selected stable clones of hJAA-F11 was put into a C2011 fibercell bioreactor (FiberCell Systems, Frederick, MD) with DMEM and 10% CDM-HD protein free serum supplement (FiberCell). Antibody purified from bioreactor harvests was purified using a MabSelect Sure HiTrap column (GE Healthcare), followed by dialysis against 50 mM sodium acetate, pH 5.5, and loaded onto a CaptoS column (GE Healthcare). Purified antibody was then eluted with a step gradient of sodium chloride.

Determination of Chemical Specificity by Printed Glycan Array

The chemical specificity of the humanized and chimeric JAA-F11 constructs were determined using the printed glycan array by the Consortium for Functional Glycomics, Emory, Ga. (<http://www.functionalglycomics.org/static/consortium/resources/resourcecoreh.shtml>) and was compared to data obtained previously for mouse JAA-F11 [27]. The method is described on the Consortium for Functional Glycomics website and is detailed by Blixt et al. [40]. The humanized JAA-F11, H2aL2a and H3L3, and chimeric constructs were analyzed for reactivity with 610 glycans at 10 μ g/ml. Data shown is for the glycans with binding to the antibody at or above 15% of the binding RFUs seen with the TF-Ag- α -Sp8.

Determination of Relative Affinity

The relative affinity binding of the humanized and chimeric JAA-F11 constructs to TF-Ag was performed using a competitive inhibition ELISA with the mouse JAA-F11 antibody. Briefly, the humanized or chimeric construct was incubated in the presence of different competing concentrations of mouse JAA-F11 on TF-Ag coated 96-well plates Immunlon plates (Thermo Scientific, Milford,

MA). Bound antibody was detected by incubation with alkaline phosphatase conjugated species specific anti-human IgG secondary antibody (Sigma, St. Louis, MO) and phosphatase substrate (Sigma, St. Louis, MO) and the absorbance reading was obtained at 490 nm. Each antibody was used at a concentration which would give an O.D. of 1.0 in our ELISA as this was in the linear portion of the curve when plotting concentration versus O.D. and thus would be in an area sensitive to inhibition. Thus H3L3 was used at a concentration of 0.02 μ g/ml, and H2aL2a was used at either 0.2 μ g/ml or 0.15 μ g/ml. Chimeric was used at either 0.3 μ g/ml or 0.25 μ g/ml. The amount of mouse antibody required to inhibit the binding of 1 μ g/mL humanized or chimeric antibodies by 50% was determined. The higher the amount of mouse antibody required for inhibition, the higher the relative affinity of the antibody. The relative affinity of each of the humanized antibodies and chimeric antibody was compared using ANOVA analysis.

Immunofluorescent Staining Detection by Flow

Single cell suspensions of *in vitro* propagated adherent cancer cell lines, MDA-Kb2, MDA-MB-231, SKBR-3, MDA-MB-453, BT549, HCC-1806, A549, and HTB-171, were removed from tissue culture flasks using Cell Stripper solution (Corning Cat# 25-056-CL). Cells were washed twice with wash buffer (DPBS/2%BSA) and suspended at 1×10^7 cells/mL in assay buffer (DPBS/2%BSA/0.04% rat IgG (Sigma Cat# 14131)) on ice bath for 30 minutes to block any sites that may non-specifically bind IgG. All staining and wash steps were performed at 4°C. After washing, 1×10^6 cells of each cell line were incubated for 60 minutes with 100 μ L of either mouse JAA-F11 monoclonal antibody at 200 μ g/mL or in assay buffer alone for controls for 60 minutes. Cells were washed twice to remove unbound antibody and 100 μ L of biotinylated rat anti-IgG3 antibody (Biolegend, Cat# 406803) at 1.5 μ g/ml was added for 30 minutes. After washing twice, 100 μ L of streptavidin-conjugated PE (Biolegend, Cat# 405204) at 0.5 μ g/ml was added for 60 minutes to detect the biotinylated anti-IgG bound to JAA-F11 on the cancer cells. After the final two washes, cells were fixed with freshly made DPBS+ 2% paraformaldehyde (Electron Microscopy Sciences Cat# 15710) and read on a BD Fortessa™ flow cytometer collecting a minimum of 10^4 cells. FCS data files were analyzed using TreeStar™FlowJo software. Humanized antibodies were diluted to 200 μ g/mL in assay buffer and Goat anti-human IgG-biotin (Vector Labs, Cat# BA3000) at 1.5 μ g/ml and stained as above.

Parallel Flow Chamber Assay. The adhesion of MDA-MB-231 cells to primary human pulmonary microvascular endothelial cells (HPMEC, ScienCell Research Laboratories, Carlsbad, CA) was studied in an *in vitro* parallel plate laminar flow chamber as follows. HPMEC were grown until 100% confluent in collagen I coated Ibidi μ -Slide VI^{0.1} for 3 days under constant perfusion with complete growth media (ScienCell, Catalog #1001) at 1 μ L/min. On the day of the experiment, the HPMEC monolayer was exposed to increasing wall shear stress levels (3.0 dyn/cm²) by perfusing MDA-MB-231 single cell suspension (5×10^4 cells/ml) in warm RPMI media containing 0.75 mM Ca²⁺, Mg²⁺ and 10.0% FBS through a precision syringe infusion/withdrawal pump KDS210 (KD Scientific, USA) for 30 minutes to activate endothelial cells [41]. Next, a single cell suspension of MDA-MB-231 cells (5×10^4 cells/ml) was perfused for a 30 minutes period at physiological shear stress (0.4 dyn/cm²) in the presence of the antibody tested or nonspecific human IgG as a control (10 mg/ml final concentration), tumor cell interactions with HPMEC were observed using an inverted phase contrast microscope Diavert, (Leitz Wetzlar,

Germany) and video recorded in at least 3 different fields for subsequent offline frame-by-frame analysis. Tumor cells that remained in the same position for at least 30 seconds were considered as stably adhered. The amount of stably adhered cells was calculated for every 5 minute interval in each observation field.

Lactate Dehydrogenase Release Cytotoxicity Assays. Antibody-dependent cellular cytotoxicity (ADCC) was determined using the lactate dehydrogenase (LDH) release assay (CytoTox 96; Promega, Madison, WI) with breast cancer cell lines according to manufacturer's protocol as previously described in Heimburg et al. [16] with some modifications. In the ADCC assays, fresh PBMCs were used as effector (E) cells, with human breast tumor target cells as target (T) cells at a 100:1 E:T ratio. Either 50 or 200 $\mu\text{g}/\text{mL}$ of humanized, mouse or chimeric JAA-F11 antibodies in phenol-red free RPMI medium was added and incubated for 17 hours. The maximum release control (target cells and medium only and lysis solution) and volume control wells (medium only) were performed. After incubation, supernatant was collected, substrate added, and LDH release was measured at 490 nm. The release of LDH from lysed cells was used to quantify cytotoxicity and expressed as the percentage of lysis. Percent cytotoxicity was calculated as $100 \times [(E - SE) / (M - SL)]$, where E is the experimental well, SE is the spontaneous release without the antibody control (target cells incubated with effector cells and PBS), M is the maximum release determined by the target cells lysed with $10\times$ lysis solution and SL is spontaneous lysis of the target cell alone. In each experiment samples were performed in quadruplicate. The data is the average from experiments that were repeated three or more times except where noted in the legend. The mouse antibody is used as a low to negative control as we had previously seen low to no ADCC with this mouse IgG₃ antibody.

Cell Internalization Assays. To address whether the antibodies can internalize into tumor cells for use as potential antibody-drug conjugates, internalization after incubation at 37°C was evaluated using ELISA and was confirmed using immunofluorescence for one of the antibodies. A quantitative two-temperature enzyme immunoassay (ELISA), to measure loss of antibody surface binding after 37°C incubation was performed as a measurement for internalization (as described in Ferguson et al. [28]). Briefly, Human breast cancer cell line (MDA-MB-231 or BT549) was tested for mouse JAA-F11, H2aL2a and H3L3 internalization. Cell lines were grown to confluence in 6-well cell culture plates. Media was decanted, and antibodies (JAA-F11 or H2aL2a or H3L3) were added at 0.2 mg/ml in 3 wells, in the 3 control wells 1 ml of media alone was added. One of the 6-well plates was incubated at 37°C and other plate 4°C. One hour after incubation the 1 ml of media alone or antibodies in media were removed and the wells were washed four times with appropriate cell culture media. After the last wash, 1 ml of freshly prepared 2% paraformaldehyde (methanol free) was added to each well and the plates were incubated for 20 minutes at RT to fix the cells without permeabilizing the cell membrane. The plates were washed four times with media, followed by 1 ml of either anti-mouse IgG (γ -chain-specific) alkaline phosphatase secondary antibody (1:5000, Sigma, St. Louis, MO) or anti human IgG (Fab specific) alkaline phosphatase secondary antibody (1:1000, Sigma, St. Louis, MO) was added and incubated at 37°C for 1 hour. Then plates were washed four times with media and 1 ml of p-nitrophenyl phosphate at 1 mg/ml was added and incubated for 1 hour at 37°C. At 1 hr., 200 microliters from each well was pipetted to a 96 well plate. Absorbencies were read at 405 nm. Unreacted substrate served as the blank. The triplicate wells were averaged, the average optical density of

the media alone blank, representing effective secondary antibody alone was subtracted from the wells containing antibody. The % internalization was given as follows:

% internalization

$$= (1 - (\text{abs } 37^\circ\text{C sample} - \text{abs } 37^\circ\text{C blank})) / (\text{abs } 4^\circ\text{C sample} - \text{abs } 4^\circ\text{C blank}) * 100$$

Controls cells with the secondary antibody conjugate followed by substrate were subtracted from the test wells. Each assay was repeated 3 or more times. The second method, used with one antibody to allow for visual confirmation of the enzyme immunoassay results, was an immunofluorescence microscopy method to qualitatively visualize internalized antibody and co-localization with lysosomal compartments, and is described as follows. Mouse 4 T1 breast cancer cells (3×10^5 cells) were seeded on coverslips in the wells of two 6-well tissue culture plates for 24 hours. Cells were then incubated with the humanized antibody H2aL2a (1 $\mu\text{g}/\text{mL}$) diluted in serum-free RPMI 1640 at 4°C for 20 minutes to allow antibody surface binding. Following the 20 minutes incubation, antibody treated media was removed from the wells and fresh serum-free RPMI media was added to one of the 6-well plates and then placed at 37°C for 60 minutes to allow internalization. The other 6-well plate was considered as the 0 minute control plate where minimal internalization takes place (maximum antibody surface binding) and this plate was kept at 4°C. After the incubation steps at 37°C and 4°C respectively, coverslips in the 6 well plates were washed twice with ice-cold 5%BSA/PBS, rinsed once with 1 \times PBS and fixed with 4% paraformaldehyde solution (Affymetrix) for 15 minutes at room temperature. After three washes in 1 \times PBS, cells were permeabilized with 0.1% Triton X-100, 0.1% sodium deoxycholate in PBS for 10 minutes at room temperature. After three rinses with 1 \times PBS, cells were incubated in 5% BSA/PBS for 30 minutes at room temperature followed by an incubation with rabbit anti-lysosomal membrane protein 1 (LAMP1; Abcam, 24,170) antibody at 1 $\mu\text{g}/\text{mL}$ in 5% BSA/PBS for 1 hour. The anti-lysosomal membrane protein was utilized as a marker for lysosomal location that would indicate internalization. After three rinses with 1 \times PBS, the coverslips were incubated with anti-human IgG-Alexa 647 and anti-rabbit IgG Alexa 488 (to detect LAMP 1) secondary antibodies (Molecular Probes, Invitrogen), at a dilution of 1:500 in 5% BSA/PBS for 1 hour at room temperature in the dark. Finally, coverslips were rinsed three times with 1 \times PBS in the dark and mounted using the Slowfade Gold reagent (Molecular Probes, Life Technologies) with DAPI. Images were taken with an AxioImager fluorescence microscope (Zeiss) and analyzed using the AxioVision Release 4.8.2 software. Images were captured using identical exposure times for both the 37°C and 4°C conditions to avoid bias. Experiments were performed at least three independent times for the humanized antibody. Color merging of the green for LAMP and the red for H2aL2a would indicate co-localization.

Preparation of the Antibody Drug Conjugate, H2aL2a-DM1

Briefly, 40 mg of hJAA-F11 human IgG1 Ab was reduced at one of the two disulfide bonds at the hinge region, with *tris*(2-carboxyethyl) phosphine (TCEP) at a 5:1 mole ratio of TCEP: IgG, for 60 minutes in a 25°C stability chamber, and gently mixed using a rotary mixer. The MC-DM1 linker payload was initially solubilized in DMSO and immediately added to partially TCEP-reduced hJAA-F11 human IgG1 Ab at a 10:1 mole ratio DM1:IgG1 to give a 15% total volume of organic solvent. The sample was gently mixed for 60 minutes in a 25°C Stability Chamber. After a 60 minute incubation, residual free thiols were

quenched with NEM at a ratio of 2:1 NEM: MC-DM1 for 30 min in a 25°C stability chamber while mixing with a rotary mixer. Next, the conjugate was purified/dialyzed overnight via four buffer changes at 150:1 ratio of dialysis buffer:conjugate into 0.1 M Potassium Phosphate pH 7.0. The conjugate was then characterized via HPLC-SEC for purity with monitoring at wavelengths of 252 nm and 280 nm; drug to antibody ratio (DAR) was determined via HIC-HPLC as well as A252/A280 ratio; SDS-PAGE (non-reducing) for purity and size; and A280 for protein concentration [42]. Each species was separated based on the surface hydrophobicity on a Tosoh TSK gel Butyl-NPR column, 4.6 mm I.D. \times 3.5 cm, 2.5 μ m (cat# 14947) at a flow rate of 1 ml/min and 20 μ L injection of samples using a 1.5 M ammonium sulfate gradient. DAR assignment was made based on elution time on column and using a reference standard as a control.

SEC-HPLC was used to assess the purity of the hJAA-F11 H2aL2a-DM1 conjugate. The Tosoh Bioscience (G3000SW \times 1) column was equilibrated with 100 mM sodium phosphate, pH 7.0, 100 mM sodium chloride, 15% isopropanol, on the Agilent 1100 HPLC column at a flow rate of 0.4 mL/min. Sample retention times were monitored at 252 nm and 280 nm.

To determine purity of the final molecule, SDS-PAGE gel electrophoresis was performed. Twenty microliters of each sample were mixed with 2 \times SDS-PAGE sample buffer (Novex, Waltham, MA) and loaded onto a 4–20% Tris-Glycine SDS-PAGE gel (Novex). Ten micrograms of full-length undigested IgG1 were loaded as reference controls. The gel was electrophoresed for 2 h at 125 V, stained for 1 h in a G250 Coomassie stain (Bio-Rad, Hercules, CA), de-stained overnight in high-purity water, and imaged using a Bio-Rad GS-800 densitometer. Blue and Mark12 Molecular Weight Markers (Life Technologies, Carlsbad, CA) were loaded onto gel as molecular-weight reference standards.

Cell Cytotoxicity In Vitro Assays

The effects of hJAA-F11-DM1 on tumor cell viability were assessed using Cell Titer-Glo reagent (Promega Corp.). Tumor cells (human breast cancer cell line: MDA-MB-231; human lung cancer cell lines: NCIH520; HTB171; A549) were plated in 96-well flat bottomed plates (1000 cells per well) and allowed to adhere overnight at 37°C in a humidified atmosphere of 5% CO₂. Cell culture medium was then removed and replaced by fresh culture medium containing different concentrations of H2aL2a-DM1, and the plates were incubated for a 5 day time period. After the 5 day time point, 10 \times Lysis buffer (Promega Corp.) was added to the appropriate positive control wells (for maximum lysis) and the plate was incubated at 37°C for 45 minutes, and then the plate was kept at RT for 30 minutes. Cell Titer-Glo reagent was added to the wells for 10 minute (2 minute on the orbital shaker) at RT and the luminescent signal was measured using a Synergy Neo2 Multi-Mode Reader (BioTek Instruments, Inc., VT, USA). IC50 was calculated using ic50.tk.

Animal Efficacy In Vivo Studies

All animal experiments were performed using IACUC approved protocols in an AAALAC approved facility. Female SCID mice, 6–8 weeks of age, were injected with 1 \times 10⁷ MDA-MB-231 cells subcutaneously, in a volume of 0.1 milliliters under the right upper abdominal nipple, under anesthesia (using Isoflurane gas) to allow careful tumor cell placement. After inoculation, tumor bearing mice were divided randomly into four groups (9 control treated with PBS, 8 mice treated with 30 mg/kg/mouse H2aL2a and 8 mice treated with

15 mg/kg/mouse H2aL2a-DM1) and treatment was initiated after 24 hour of tumor cell inoculation. Each mouse was injected intraperitoneally (I.P.) on day 1, 4, 7 and then one injection per week for 5 weeks. Tumor size was measured once every 3 days with a surgical vernier caliper. At the end of the experiment (on day 50), the mice were anesthetized with isoflurane gas and sacrificed. Tumors from each mouse were removed, measured with the digital caliper and weighed individually. Lungs, heart and liver were viewed for gross determination of metastasis for each mouse.

For the second *in vivo* experiment, a few changes were made to the above protocol; a pretreatment was done by adding 3 mg/mouse of rabbit immunoglobulin I.P. to the MDA-MB-231 bearing mice on day 6, and the antibody treatment of the mice did not begin until day 7, and in addition fewer treatments were done, for a total of 6 weekly treatments for each group. The tumor bearing mice were divided randomly into three groups (10 control treated with PBS, 10 mice treated with H2aL2a, 30 mg/kg/mouse, and 10 mice treated with H2aL2a-DM1, 15 mg/kg/mouse). Each mouse was injected intraperitoneally on day 7 and weekly thereafter for 5 weeks. Tumor size was measured once every 3 days with a surgical vernier caliper. At the end of the experiment (on day 50), the mice were anesthetized with isoflurane gas and sacrificed. Tumors from each mouse were removed, measured with the digital caliper and weighed individually. Lungs, heart and liver were viewed for gross determination of metastases for each mouse.

Statistical Analysis

Unpaired Student's t-test and ANOVA analysis with Dunnett's were utilized for statistical evaluation as described in the Figure legends. *P* values <.05 were considered statistically significant.

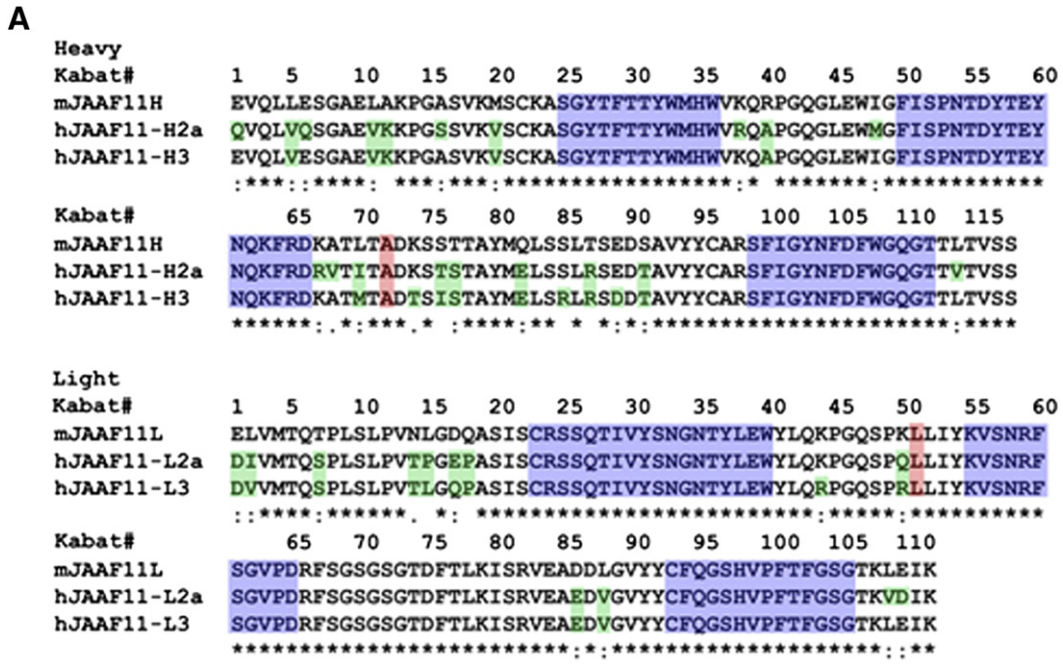
Immunohistochemistry

Tumors from mice were removed on day 50 and placed into Z-fix for 24 hours, followed by 70% ethanol. Tumors were then embedded in paraffin. Slides were deparaffinized by passing them through xylene, 100% ethanol, 95% ethanol, 70% ethanol, followed by water. Slides were washed twice with Tris-phosphate wash buffer and endogenous peroxidases were blocked with 3% hydrogen peroxide in methanol for 15 minutes. Slides were then washed and endogenous biotin was blocked with an avidin-biotin blocking kit (Thermo Scientific). Following blocking with a 2.5% goat serum (Vector Labs), slides were incubated with either goat serum alone or biotinylated anti-human IgG antibody (Vector Labs) in goat serum for 30 minutes. Following washing, slides were treated using a Vectastain Elite ABC reagent (Vector Labs) for 30 minutes, then washed and developed with ImmPact DAB chromogen (Vector Labs). Slides were counter stained with Modified Harris Hematoxylin (Richard-Allan Scientific), dehydrated and then mounted. Slides were then scanned and images taken using an Aperio Scan Scope GL (Leica BioSystems).

Results

The Designed Humanized JAA-F11 Antibody Constructs

After the sequences of the mouse JAA-F11 variable regions were verified, the CDRs for humanized JAA-F11 were defined so as to maintain specificity and affinity for TF-Ag. The inclusive CDRs were defined according to both Kabat et al. [36] and Chothia et al. [37] based on sequence and structural variability, respectively. X-ray crystallography and computational carbohydrate threading studies on mouse JAA-F11 [38] identified amino acid residues within 5 to 6 Å from the binding site. These amino acids as well as cysteine residues at



B

JAA-F11 Variants	T20-score (FR & CDR)		T20-score (FR)	
	Heavy Chain	Light Chain	Heavy Chain	Light Chain
Chimeric	67	78	72	86
H2aL2a	80	83	93	95
H3L3	79	86	87	94

Figure 2. Amino acid sequence alignments of mouse (mJAA-F11) with humanized H2aL2a and H3L3 antibody and immunogenicity assessment of the H2aL2a and H3L3. A) Amino acid sequence alignments of mJAA-F11 heavy (top) and light (bottom) chain variable regions with variable regions of H2aL2a and H3L3 constructs. Green indicates the differences among the humanized antibodies and mJAA-F11. Alanine at position 71 (top) and Leucine at position 46 (bottom) shaded pink, indicate mouse residues that were retained to avoid steric clashes. The CDRs are shaded blue. Numbering is according to Kabat. B) Assessment of immunogenicity of the H2aL2a and H3L3 constructs by using the scoring system developed by Gao et al. [39]. T20 score is used to measure “humanness” of monoclonal antibody variable region sequences; T20 score > 80 for FR and CDR sequences is not immunogenic in humans; T20 score > 85 for FR sequences only is not immunogenic in humans (see main text for details). The closer the number is to these cut-offs the less immunogenic the antibody. FR = framework; CDR = complementarity determining region.

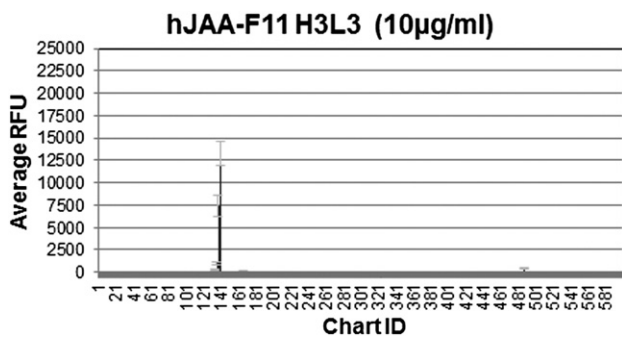


Figure 3. Binding of H3L3, H2aL2a and chimeric antibodies on a CFG glycan array. The arrays contained 440 glycans (mouse) and 601–610 glycans (chimeric and humanized). Sample RFU vs. glycan binding is shown for H3L3 since these graphs are so similar. Only TF-Ag and 3 or 4 related saccharides bound to the antibodies, and these are not seen in normal human tissue.

Gal, forming GlcNAcβ1–3Galβ1–3GalNAcα-, or by a 2–3 sialyltransferase forming Neu5Acα2–3Galβ1–3GalNAc (sialyl-TF) or with a second sialyltransferase forming Neu5Ac2–3Galβ1–3(Neu5Acα2–6)GalNAc (disialyl-TF). All of these structures show no binding to the mouse [27,38], chimeric or the humanized JAA-F11 constructs. Thus, normal tissue binding is not expected for JAA-F11 or the humanized hJAA-F11 antibodies. At 10 µg/ml the chimeric JAA-F11, and hJAA-F11 H2aL2a and H3L3 antibodies bind to an additional two

Table 1. Example RFU Graph Showing High Degree of Specificity of These Antibodies.

Chart ID	Saccharides of 601 Tested With ≥15% Binding to Any of the Antibodies	H3L3 Average RFU	H2aL2a Ave RFU	Chimeric Ave RFU
139	Galb1–3GalNAcα-Sp8	13,343	21,619	13,860
137	Neu5Acβ2–6(Galβ1–3)GalNAcα-Sp8	7391 (55%)	25,576 (118%)	5390 (38%)
135	Neu5Acα2–6(Galβ1–3)GalNAcα-Sp8	1016 (8%)	6921 (32%)	3240 (23%)

Saccharides shown if RFU ≥15% of Galβ1–3GalNAcα-Sp8 value for any construct.

Table 2. Four Similar TF-Ag Related Structures on Normal Tissues

The Glycan Array Data Showed that the Humanized hJAA-F11s and Chimeric JAA-F11 Antibodies do not Bind Gal β 1-3GalNAc-Beta (β) Linked Structures and Also Common Elongation Structures on Normal Tissues. RFU Refers to Relative Fluorescence Unit.

Glycan Array #	Glycan Structure	Linker	H3L3 RFU	H2aL2a RFU	Chimeric RFU
^a 144	Gal β 1-3GalNAc β 1-4(Neu5Ac α 2-3)Gal β 1-4Glc β -	Sp0	10	7	-1
^b 145	Gal β 1-3GalNAc β 1-4Gal β 1-4Glc β -	Sp8	15	29	28
^c 88	GlcNAc β 1-3Gal β 1-3GalNAc α -	Sp8	19	49	78
^d 223	Neu5Ac α 2-3Gal β 1-3GalNAc α -	Sp8	11	22	109

All RFU on these saccharides are <1% of the reaction with the TF-Ag alpha disaccharide-Sp8.

^a Glycan #144 is ceramide ganglioside GM1 found on brain and red blood cells.

^b Glycan #145 is ceramide asialo-GM1 found on NK cells, kidneys, spleen, and regenerating respiratory epithelial cells.

^c Glycans # 88 and #223 are common elongation structures on normal tissues.

^d Glycans # 88 and #223 are common elongation structures on normal tissues.

saccharides out of the 610 saccharides tested (Figure 3). However, neither of the additional binding saccharides are expected to be a problem biologically for tumor targeting with hJAA-F11. The Neu5Ac β 2-6 Gal β 1-3GalNAc is not a natural structure in humans. The other structure, Neu5Ac α 2-6(Gal β 1-3)GalNAc β , has only been reported in respiratory mucin of a bronchiectasis patient [44], human midcycle cervical mucin [45], human chorionic gonadotropin [46] and meconium, all that should not affect therapeutic use.

hJAA-F11 Constructs have Improved Relative Affinity to TF-Ag

The relative binding affinities of the hJAA-F11 constructs and chimeric antibodies to TF-Ag were determined by comparing the ability of the mouse antibody to compete with the antibodies in an enzyme immunoassay. In this assay, the humanized or chimeric Ab is mixed with serial dilutions of the mouse anti TF-Ag antibody (mJAA-F11). Binding of the human or chimeric anti-TF-Ag to the TF-Ag coated plate is measured using a species-specific anti-human

Table 3. Relative Affinity for TF-Ag: μ g mJAA-F11 Required for 50% Inhibition of μ g of hJAA-F11 (Chimeric, H2aL2a & H3L3) Antibody. The Average of at Least Three Independent Experiments are Shown \pm Standard Deviation.

H2aL2a (μ g)	H3L3(μ g)	Chimeric(μ g)
1.9 \pm 0.3	33.3 \pm 6.4****	0.87 \pm 0.2

IgG. The amount of mouse mJAA-F11 antibody that is required to inhibit 1 μ g of hJAA-F11 or chimeric antibody to 50% is extrapolated and taken as a measure of relative affinity. Inhibition curves are shown in Figure 4. The higher the amount of mouse antibody required for inhibition, the higher the relative affinity of the antibody. The results are summarized in Table 3. This table shows the half maximal inhibitory concentration of mouse JAA-F11 required to compete with 1 μ g of this hJAA-F11 antibody. hJAA-F11 H3L3, and H2aL2a antibody showed higher relative affinity to TF-Ag with a relative affinity of 33.32 \pm 6.4, and 1.95 \pm 0.3 relative to the mouse antibody, while the chimeric antibody with a half maximal inhibitory concentration of 0.81 \pm 0.21 relative to the mouse antibody has a similar affinity as the mouse antibody as would be predicted since it has the same variable region (Figure 4B). Both humanized antibodies have a significantly higher relative affinity than the chimeric, $P < .01$. Therefore, both humanized JAA-F11 constructs displayed better binding to TF-Ag than the original mouse antibody. Next, we wanted to investigate the biological activity of both of these humanized JAA-F11 antibodies.

Flow Cytometric Analysis of TF-Ag Expression On Human Cancer Cell Lines with mJAA-F11, and hJAA-F11 Constructs H2aL2a and H3L3

Multiple breast and lung cancer cell lines were examined by flow cytometry using mJAA-F11 to determine relative TF-Ag expression

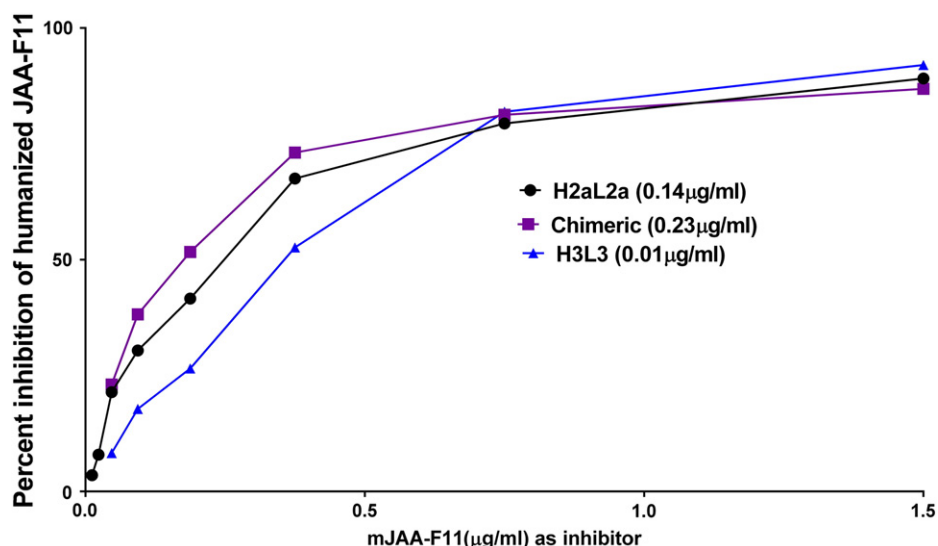


Figure 4. The humanized H3L3 has a higher affinity than H2aL2a antibody which has a higher affinity than chimeric antibody to TF-Ag-BSA. A) Graph shows relative affinity of H2aL2a and chimeric antibodies to TF-Ag as determined by ELISA. Each antibody was mixed with serial dilutions of mJAA-F11 and binding to the TF-Ag coated plate was measured by using a species-specific alkaline phosphatase anti-human IgG antibody. The amount of mJAA-F11 antibody required to inhibit 1 μ g of each tested antibody (H3L3, H2aL2a, and chimeric antibodies) to 50% was extrapolated and is depicted in the table (B). The higher the amount of mouse antibody required for inhibition, the higher the relative affinity of the antibody. ANOVA analysis was performed on the relative affinity (IC_{50}) values obtained for each antibody tested (as described above) and binding of H3L3 was significant at $P < .001$ (****). Humanized and chimeric antibodies used at a concentration which would yield an O.D. of 1.00 in the EIA when not inhibited. H3L3 used at \sim 10 times the H2aL2a concentration and \sim 15 times the chimeric concentration.

levels. The relative expression of TF-Ag for the human breast cancer cell line MDA-MBA-231, is compared to other breast (Figure 5A) and lung cell lines (Figure 5B). The breast cell lines in order of TF-Ag expression are; BT549, and HCC1806 (both high expressers), MDA-MB-453

(moderate expresser), and SKBR3, MDA-MB-468, MDA-MB-231, MDA-MB-kb2, and Du4475 (low expressers) (Figure 5A). The two lung cancer cell lines tested are the adenocarcinoma line A549, and a small cell lung cancer cell line, HTB-171 (Figure 5B) which show low

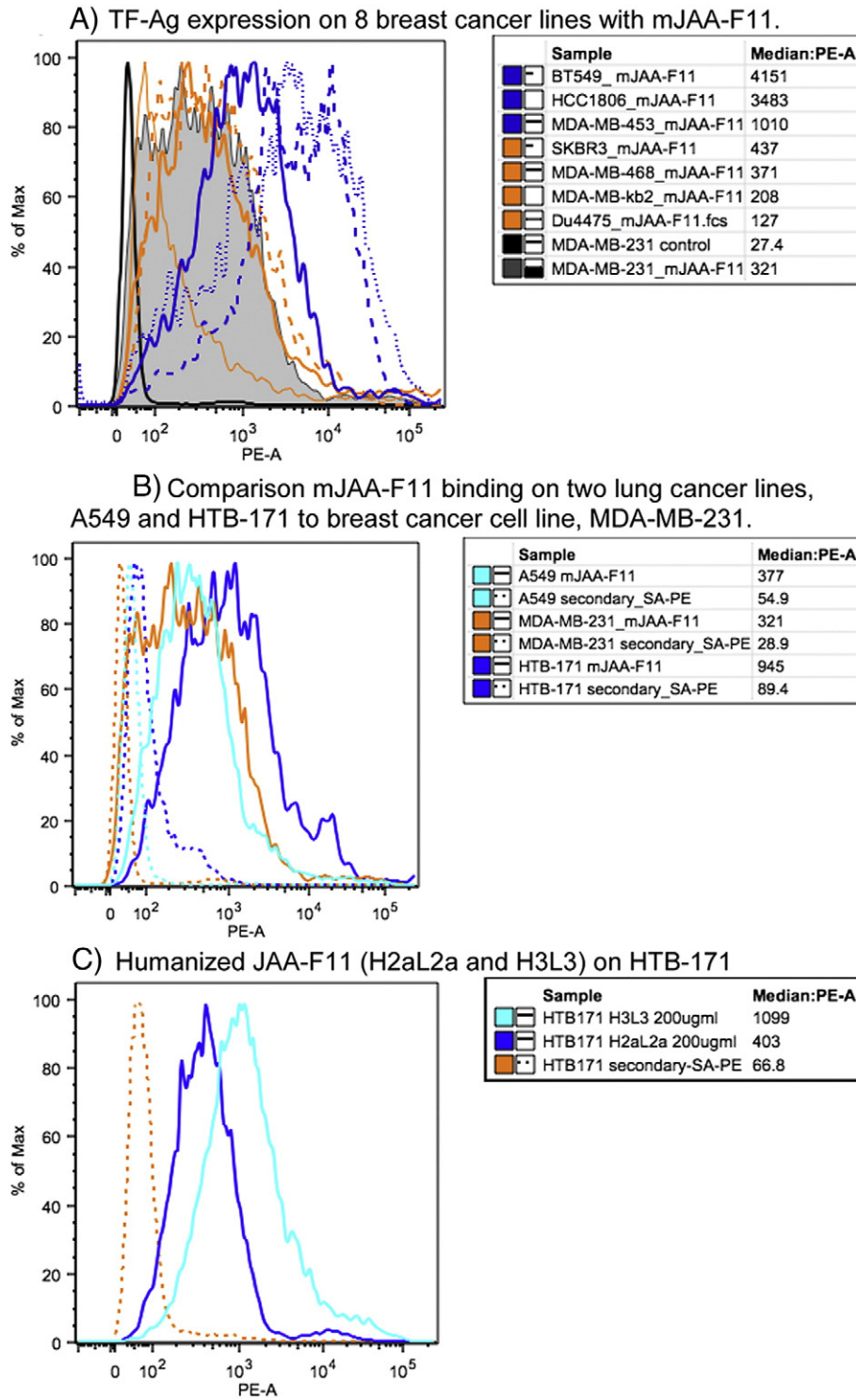


Figure 5. Flow cytometric analysis of TF-Ag Expression on Human Cancer cells. Flow histograms showing A) Relative TF-Ag expression levels on eight breast cancer cell lines BT549, HCC-1806, MDA-MB-453, SKBR-3, MDA-MB-468, MDA-MB-231, MDA-MB-kb2 and Du4475 detected with mJAA-F11 using rat anti-mouse IgG3-biotin/Streptavidin-PE. Solid black line is used to show the relative background with secondary antibody alone for MDA-MB-231. B) Relative TF-Ag expression levels on the breast line MDA-MB-231 compared to the lung cancer cell lines A549 and HTB-171, detected with mJAA-F11 using rat anti-mouse IgG3-biotin/Streptavidin-PE and C) binding of hJAA-F11 constructs H2aL2a and H3L3 to HTB-171 detected with Goat-anti-human IgG-biotin/Streptavidin-PE. Solid lines binding of JAA-F11 or hJAA-F11 antibody; dashed lines background binding with detection system only.

and moderate expression respectively. Figure 5C, illustrates the relative ability of hJAA-F11 constructs to bind HTB-171 cells. H3L3 binding is higher (MFI 1099) to TF-Ag on HTB-171 cells compared to H2aL2a binding (MFI 403) under the same conditions using a goat anti-human IgG-biotin/Streptavidin-PE detection system. These results indicate that both hJAA-F11 antibodies can also be used to assess TF-Ag surface expression on cell lines.

hJAA-F11 Prevents MDA-MB-231 Cellular Adhesion to Normal Human Endothelial Cells

TF-Ag is an important player in the adhesion of cancer cells to normal human cells, through the interaction of TF-Ag with the cellular lectin Galectin-3 [47,48]. This mechanism is considered one of the hallmarks of metastasis as cancer cells bearing TF-Ag are thereby able to transverse from the primary tumor site and bind to the vasculature in a distal site to initiate the formation of secondary tumors. An antibody that binds TF-Ag would feasibly be able to prevent metastasis by blocking the TF-Ag interactions with vascular cells. To address this possibility, a well-established parallel flow chamber assay was used to investigate the ability of hJAA-F11 to block metastasis-associated adhesion of human cancer cells to primary human microvascular endothelial cells [13,18,20,47,48]. This assay has been previously used to demonstrate that TF-Ag interactions with endothelium expressed galectin-3 are critical for mediating metastatic cell adhesion to endothelium under physiological flow conditions. Using this assay, TF-Ag positive metastatic human breast carcinoma cells MDA-MB-231 were passed over the monolayer of primary normal human pulmonary endothelial cells under physiological conditions. The cells were treated with either control IgG, or anti-TF-Ag antibody (mouse JAA-F11 or hJAA-F11) and the cell adhesion was assessed by video microscopy. In the presence of control IgG, MDA-MB-231 strongly adhered to normal endothelial cells (Figure 6), however, in the presence of either JAA-F11 or hJAA-F11 H2aL2a, cancer cells were prevented from adhering to endothelial cells through the blocking of TF-Ag by either the original mouse or humanized JAA-F11 antibody. Further, it appears that the humanized H2aL2a had improved blocking ability compared with the original mouse antibody. This is strong evidence that the humanized hJAA-F11 can be used to block tumor cell metastasis-associated adhesive interactions and potentially prevent metastasis, which will be further investigated in future studies.

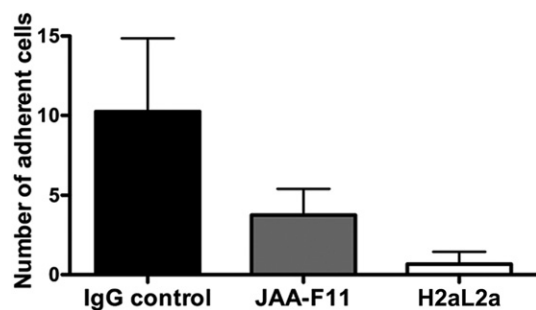


Figure 6. Anti-metastatic effect of mouse JAA-F11 and hJAA-F11 in an *in vitro* model. Graph comparing humanized JAA-F11 H2aL2a, and JAA-F11 effect on adhesion of MDA-MB-231 to primary pulmonary microvascular cells. ANOVA analysis differences are highly significant ($P < .0001$). Adherent cells are those that stay attached to the microvascular cells for at least 30 seconds.

Effector Functions of hJAA-F11

In vivo efficacy of antibody immunotherapy might involve many different mechanisms including the immunologic effector functions of the Ab. Therefore, the ability of the humanized antibody to carry out ADCC was determined using multiple human cancer cell lines (Figure 7). At 200 $\mu\text{g/ml}$, H2aL2a was effective in ADCC killing against NCI-H520, BT549, HTB-171, and MDA-MB-231; while chimeric antibody showed little ADCC activity even at the 200 $\mu\text{g/ml}$ concentration (<20% cytotoxicity) (Figure 7A). Mouse JAA-F11, as a negative or low antibody was also compared with H2aL2a and these results are shown in Figure 7. Figure 7B shows that at 50 $\mu\text{g/ml}$, H3L3 facilitated statistically more ADCC than H2aL2a on all cell lines tested. Even at the lowered concentration, H2aL2a still caused lysis of ~20% of both the NCI-H520 and BT549 cells, whereas at 50 $\mu\text{g/ml}$ H3L3 caused >50% kill of NCIH520, close to 50% kill of BT549 and MDA-MB-231, and ~30% kill of HTB-171 with the same effector to target ratio. This indicates that hJAA-F11 antibody constructs have potential for naked antibody immunotherapy.

Humanized hJAA-F11 Internalizes Into Cancer Cells

Since antibodies can potentially be used to covalently carry drugs or toxins in the form of antibody-drug conjugates into cells, internalization is an important aspect to analyze. Internalization of humanized and chimeric JAA-F11 into 4 T1 breast tumor cells was determined by two methods, first an enzyme immunoassay with surface binding of antibody measured and compared after incubating the cells for 1 hour at either 4°C or 37°C and detection without a permeabilization step (Figure 8A). The second method was an immunofluorescence microscopy method with surface staining for hJAA-F11 followed by permeabilization and internal staining for hJAA-F11 and anti-LAMP-1 (lysosomal associated membrane protein, a lysosomal marker) and DAPI (nuclear) staining (Figure 8B). Mouse JAA-F11 had previously been shown to internalize within 1 hour at 37°C by the enzyme immunoassay method [28]. In the enzyme immunoassay, the majority of mouse JAA-F11, chimeric, H2aL2a, and H3L3 antibodies were shown to internalize into the human breast cancer line MDA-MB-231 (Figure 8A), with H3L3 internalizing to the highest extent of the 3 antibodies. In the immunofluorescence microscopy experiments, H2aL2a is analyzed to give a visual conformation of the enzyme immunoassay results. In agreement with the enzyme immunoassay, the majority of H2aL2a antibody showed internalization and co-localization with the lysosomal protein marker, LAMP-1, in the MDA-MB-231 cell line (Figure 8B). Therefore, both assays confirm that these antibodies internalize.

Antibody-Drug Conjugate (ADC) Characterization and In Vitro Cytotoxicity

Many current targeted therapies now rely on conjugating potent (but relatively nonspecific) anti-cancer drugs directly to a specificity factor in the form of an antibody. Therefore, as proof-of-principle for hJAA-F11 as the antibody in an ADC, the microtubulin inhibitor DM1 ($\text{N}^{2'}$ -Deacetyl- $\text{N}^{2'}$ -(3-mercapto-1-oxopropyl) maytansine) was conjugated to hJAA-F11 H2aL2a with a pH sensitive linker that would release the payload upon internalization and acidification within the lysosome. The site directed conjugation of MC-DM1 (maleimidocaproyl- $\text{N}^{2'}$ -Deacetyl- $\text{N}^{2'}$ -(3-mercapto-1-oxopropyl) maytansine) to partially TCEP (tris(2-carboxyethyl) phosphine), which reduces solvent exposed disulfides, reduced hJAA-F11 Ab, resulting in an ADC with an average DAR of 3.54 as determined via

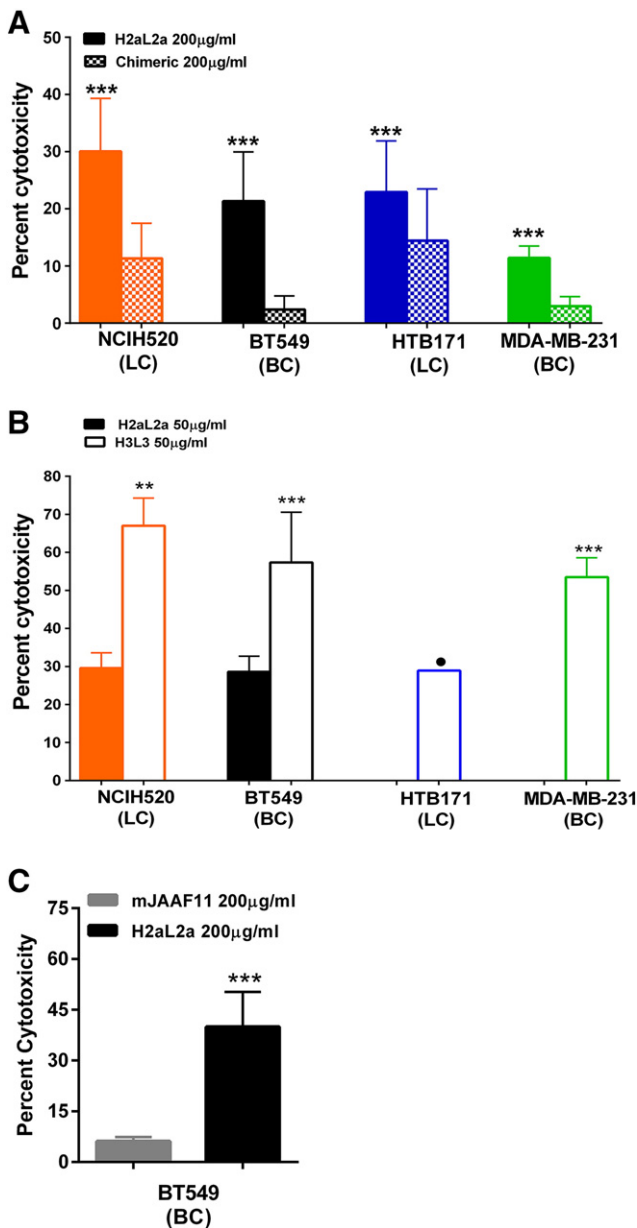


Figure 7. ADCC activity versus TF-Ag positive breast and lung cancer cell lines by 7a) H2aL2a and chimeric antibodies at 200 µg/ml, and 7b) H3L3 and H2aL2a Ab at 50 µg/ml. A) 200 µg/ml of the H2aL2a and chimeric were used in ADCC assays against several human cancer cell lines. BC indicates a breast cancer line, while LC indicates a lung cancer line. H2aL2a was most effective in ADCC against NCI-H520, then in decreasing amounts towards BT549, HTB-171, and MDA-MB-231, and the chimeric antibody showed little ADCC even at this 200 µg/ml concentration ($P < .05$) B) 50 µg/ml of either H2aL2a or H3L3 were used in ADCC assays against several human cancer cell lines. C) 200 µg/ml concentrations of either H2aL2a were added to BT549 cells. The mouse JAA-F11, effectively a negative control antibody did not show appreciable ADCC even at 200 µg/ml with the BT549 cells. In the HTB-171 and MDA-MB-231 cell lines with H2aL2a, there was no appreciable ADCC activity above background and was not graphed. • indicates significance differences in one representative experiment. ** indicates significance in two of three independent experiments. *** indicates significance across all three independent experiments.

mole ratio of DM1:Ab by A252/A280 and a DAR of 2.12 as determined by HIC-HPLC peak integration, with the predominant species being a DAR of 2 as determined via HIC-HPLC (Figure 9) [42]. HIC-HPLC was used to determine the DAR of the hJAA-F11 DM1 conjugate based on the elution time of each individual species contained within the conjugate [27]. Furthermore, the hJAA-F11 conjugate was greater than 93% pure as determined via SEC-HPLC.

Using an *in vitro* cell culture approach, the sensitivity of various human cancer cell lines to DM1 conjugated hJAA-F11 was analyzed. Several well studied triple negative human breast cancer (TNBC) lines (MDA-MB-231, MDA-MB-468, and MDA-MB-453) were treated. Increasing amounts of hJAA-F11-DM1 was titrated with each cell line and after 5 days, the cell viability was determined. All three TNBCs showed sensitivity to hJAA-F11-DM1, with MDA-MB-468 having an IC₅₀ of 0.01 µg/mL hJAA-F11-DM1, MDA-MB-453 with an IC₅₀ of 1.2 µg/mL and MDA-MB-231, the least sensitive, having the highest IC₅₀ at 2.1 µg/mL (Figure 9B). A similar experiment using only naked hJAA-F11 showed no discernable killing of MDA-MB-231 (data not shown), indicating that the specific delivery of DM1 through hJAA-F11 was responsible for cancer cell killing. TF-Ag is also present on many carcinoma types, including non-small cell lung cancer (NSCLC) and small cell lung cancer (SCLC). To determine the feasibility of using hJAA-F11-DM1 for lung cancer therapy, we tested TF-Ag positive lung cancer lines SCLC HTB-171 (NCI-H446) [49,50] and the TF-Ag positive NSCLC squamous cell carcinoma NCI-H520 (HTB-182) [51] and the NSCLC adenocarcinoma A549 [52,53]. While all the lines showed sensitivity to hJAA-F11-DM1, the medium TF-Ag expressing HTB-171 was more sensitive (IC₅₀ 0.34 µg/mL), followed by NCI-H520 (IC₅₀ 1.35) and the lower TF-Ag expressing A549, showed sensitivity similar to the breast cancer line MDA-MB-231 (IC₅₀ 2.1 µg/mL) (Figure 9C). HIC-HPLC was used to determine the DAR of the hJAA-F11 DM1 conjugate based on the elution time of each individual species contained within the conjugate [27]. In conclusion, hJAA-F11-DM1 also shows promise as a lung cancer therapy, which will be focused on more fully in a future study.

In Vivo Efficacy of hJAA-F11 and hJAA-F11-DM1

As hJAA-F11-DM1 showed the ability to kill the human TNBC cell line MDA-MB-231 in culture, the ability of drug conjugated hJAA-F11 to kill tumor cells in the *in vivo* mouse xenograft model was addressed (Figure 10). Even though this cell line has low TF-Ag expression (Figure 6), it was chosen for the *in vivo* analysis because it is a human triple negative model, and is one of the most widely used breast xenograft models. In the first *in vivo* experiment (Figure 10), mice were inoculated with MDA-MB-231 cells and 24 hours later treatment was initiated, including a control group treated with PBS, and experimental groups treated with hJAA-F11 H2aL2a at 30 mg/kg, and a group treated with H2aL2a-DM1 at 15 mg/kg. Treatments were administered i.p. on day 1, 4, 7 and thereafter once per week for 5 weeks. Tumor size was measured once every 3 days, and on day 50, the mice were sacrificed, and tumors were removed, measured and weighed. Figure 10 panels A and B show the early effect of both 30 mg/kg hJAA-F11 (statistically smaller at day 30) and 15 mg/kg hJAA-F11-DM1 conjugate (statistically significant from day 25–30, and day 42–day 50). Panels C and D show the tumor volume data to day 50 and the tumor weight data at day 50, respectively. The hJAA-F11-DM1 conjugate causes a statistically significant difference in both of these measurements at day 50.

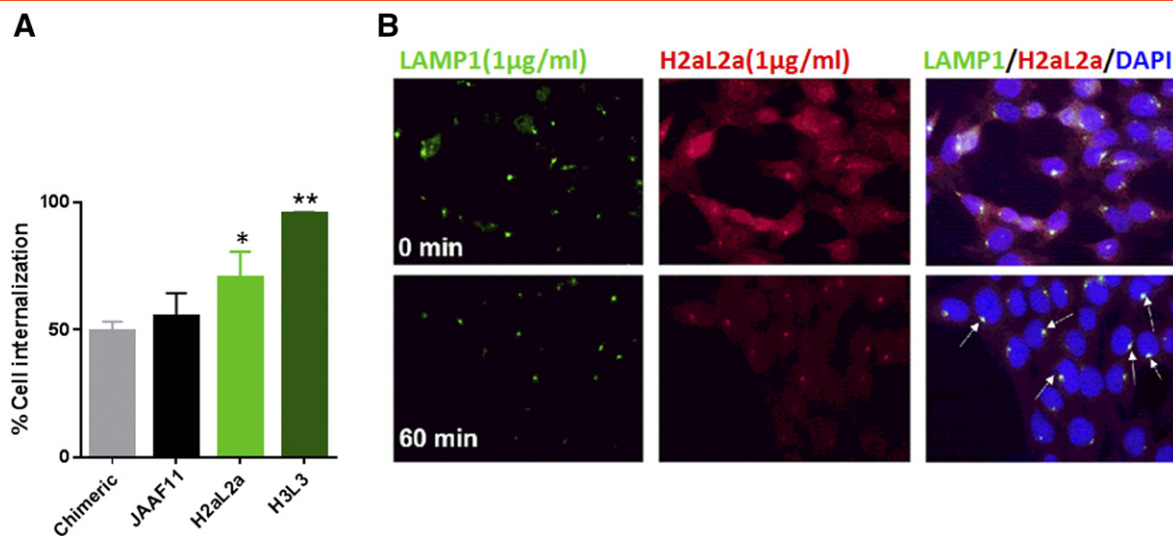


Figure 8. Internalization of H3L3 and H2aL2a antibodies in 4 T1 and MDA-MB-231 cells. A) Internalization by EIA detection of antibody surface binding following incubation of cells with antibody at 4°C (no internalization) and 37°C degrees (to induce internalization). All antibodies displayed internalization, where H2aL2a displayed significantly more internalization than chimeric (*, $P < .05$) and H3L3 showing significantly more internalization compared to all antibodies (**, $P < .05$). Bars represent mean \pm S.E. ($n = 3$ experiments). B) Representative images showing immunofluorescent staining of Ab H2aL2a and the lysosomal protein marker, LAMP-1 (green). Top panels MDA-MB-231 cells were pre-incubated with antibody (1 μ g/mL) for 20 min at 4°C. Lower panels after at 37°C for 60 min. Merged images confirm internalization of H2aL2a and lysosomal co-localization with LAMP-1 in merged images (arrows). Total magnification was 40 \times .

The above experiment was repeated with two modifications, a pretreatment with 3 mg/mouse of rabbit IgG was utilized to block Fc receptors in the SCID mice, and the first injection of antibody was delayed to day 7 after tumor implantation and continued weekly. In Figure 11A, both H2aL2a and H2aL2a-DM1 inhibited growth statistically as measured by tumor volume from day 38 to the completion of the study. The tumor volumes of both the naked H2aL2a and the H2aL2a-DM1 conjugate treated mice were significantly decreased relative to the control treated mice at time points indicated by the asterisks. At day 50, tumors were removed and while the volumes of the removed tumors remained significantly different, tumor weight only approached significance ($P = .0506$) in the H2aL2a-DM1 group (Figure 11B). Figure 12 shows that after I.P. injection hJAA-F11 can be detected in the tumor of a SCID mouse by IHC after hJAA-F11 treatment confirming the role of the humanized antibody in the efficacy data. Even though this xenograft model system was not optimized for hJAA-F11 therapy since MDA-MB-231 has low to moderate TF-Ag expression, and the H2aL2a is of lower affinity than the more recently acquired H3L3, H2aL2a-DM1 and naked hJAA-F11 antibody have potential as adjunct therapy for TNBC.

Discussion

TF-Ag, the disaccharide tumor antigen targeted by JAA-F11, has been studied for many years, and there is strong evidence concerning its tumor associated presence on ~80% of carcinomas and lack of expression in normal tissues [1–10]. It is an adhesion molecule related to invasiveness, so use of an antibody targeting this molecule has potential as an immunotherapeutic, as an antibody-drug conjugate for direct tumor cell killing and for blocking metastasis. Another unique feature of TF-Ag as a target is that patients have naturally occurring antibodies to TF-Ag, and these antibody levels are positively correlated with prognosis without causing any autoimmunity [1,54–56] indicating low potential toxicity. Thus, hJAA-F11

constructs have great potential to be well tolerated in adjunct cancer therapy. Humanized JAA-F11 antibodies can also be developed for tumor localization, since TF-Ag is not secreted and thus not present in the serum. This has been supported by mouse 124 I-JAA-F11 imaging studies in syngeneic and xenogeneic tumor models in mice, where long tumor retention time was observed [27].

What makes the patented JAA-F11 antibody unique for this antigen is its high degree of specificity, in that it reacts to the unsubstituted Gal β 1–3GalNAc alpha linked to serine (the true tumor TF-Ag), and not to the Gal β 1–3GalNAc beta structure in glycolipids which is on some normal tissues including the kidney. By developing humanized JAA-F11 constructs through careful inclusive use of Kabat and Chothia guidelines as well as crystallography and computational carbohydrate threading (an innovative additional step) to determine the CDRs, we maintained or enhanced antibody specificity and affinity (Figures 3 and 4 and Tables 1-3). The affinity and the specificity of the humanized antibody for the antigen were fully retained or improved when compared to its mouse and chimeric counterpart. Through use of the top 10 most similar human antibodies in the construction of the humanized antibodies, we were able to obtain two hJAA-F11 constructs (H2aL2a and H3L3) with T20 scores [39] that indicate little to no immunogenicity (Figure 2B), suggesting promising immunotherapeutic properties. The humanized hJAA-F11 antibodies H2aL2a and H3L3 showed promising ADCC properties, significantly inducing breast and lung cancer cell killing *in vitro* when compared to the chimeric antibody and the mouse antibody (Figure 7). This ADCC improvement in the switch from a mouse IgG3 to a human IgG1 is similar to that seen by Cheung et al. with their anti-GD2 antibody [57]. In addition, hJAA-F11 H2aL2a was shown to reduce tumor growth in a mouse xenograft human triple negative breast cancer model (Figures 10 and 11).

Importantly, the chimeric and humanized hJAA-F11 H2aL2a and H3L3 antibodies were also shown to internalize rapidly, with 68–95% of the antibody being internalized within 1 hour (Figure 8),

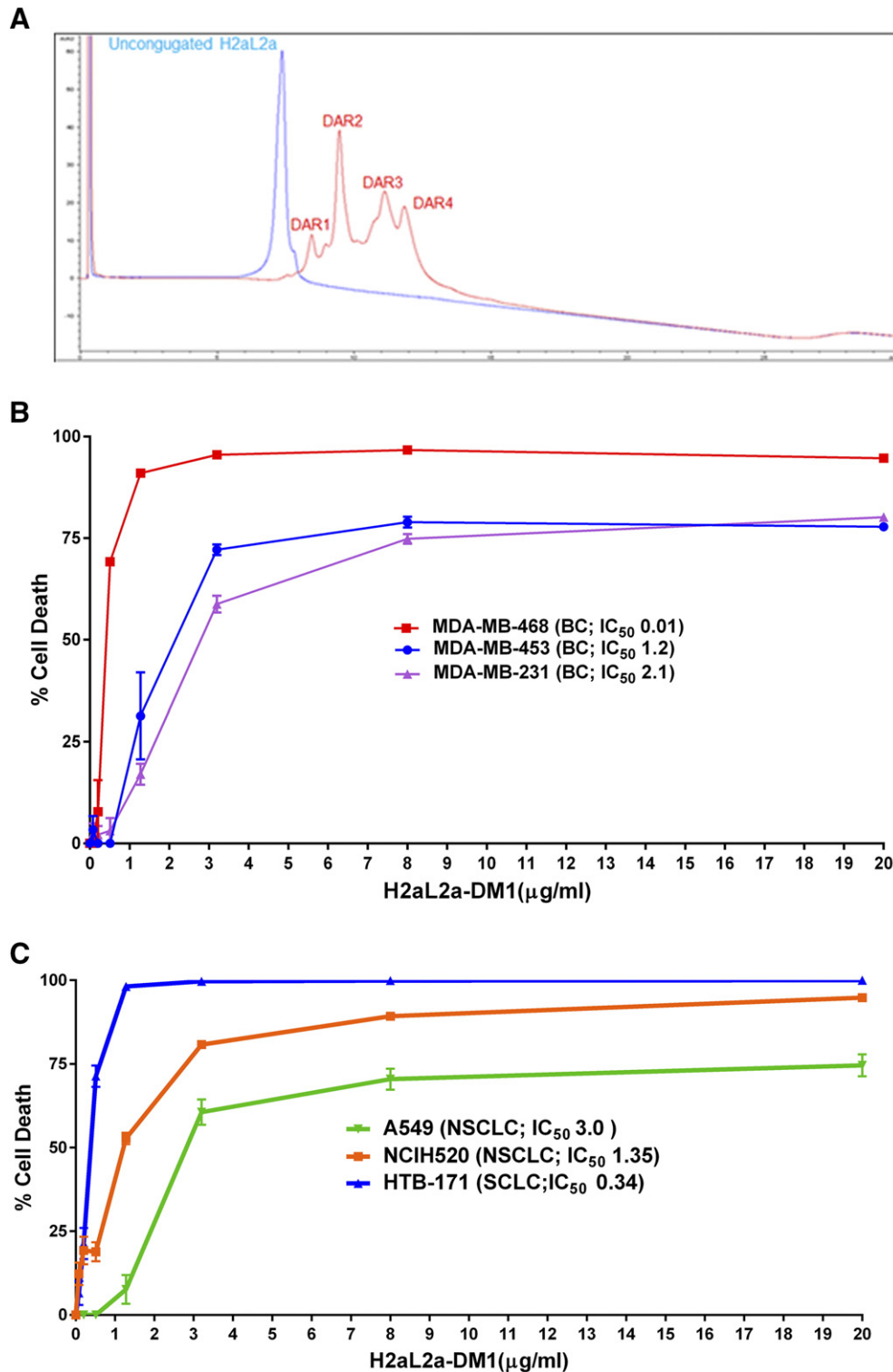


Figure 9. Characterization of Maytansine (DM1) Conjugate of H2aL2a. A) H2aL2a-DM1 conjugate production. HIC-HPLC Chromatogram of H2aL2a Ab and H2aL2a-DM1 conjugate at A280. B) *In vitro* cell efficacy against human breast cancer (BC) cell lines using H2aL2a-DM1. C) *In vitro* efficacy against human lung cancer cell lines using H2aL2a-DM1. NSCLC is a non-small cell lung cancer and SCLC is a small cell lung cancer. B) & C) DM1 conjugated H2aL2a antibody showed enhanced anti proliferative activity on TF-Ag positive breast and lung cancer cell lines. All experiments were carried out to Day 5 of treatment and cell viability detected using a Cell-Glo reagent. (IC₅₀ values, $\mu\text{g/mL}$ H2aL2a-DM1).

comparable or improved when compared to the mouse JAA-F11 antibody [28]. This observation led to construction of our proof of principle ADC, hJAA-F11-DM1 conjugate which was shown to have potent *in vitro* cytotoxic activity in several human breast and lung

cancer cell lines that showed varying TF-Ag expression (Figures 6 and 9B). Initial *in vivo* efficacy studies also demonstrated that hJAA-F11-DM1 conjugate reduced tumor growth (volume and weight) in a mouse xenograft human triple negative breast cancer model (Figures 10 and 11).

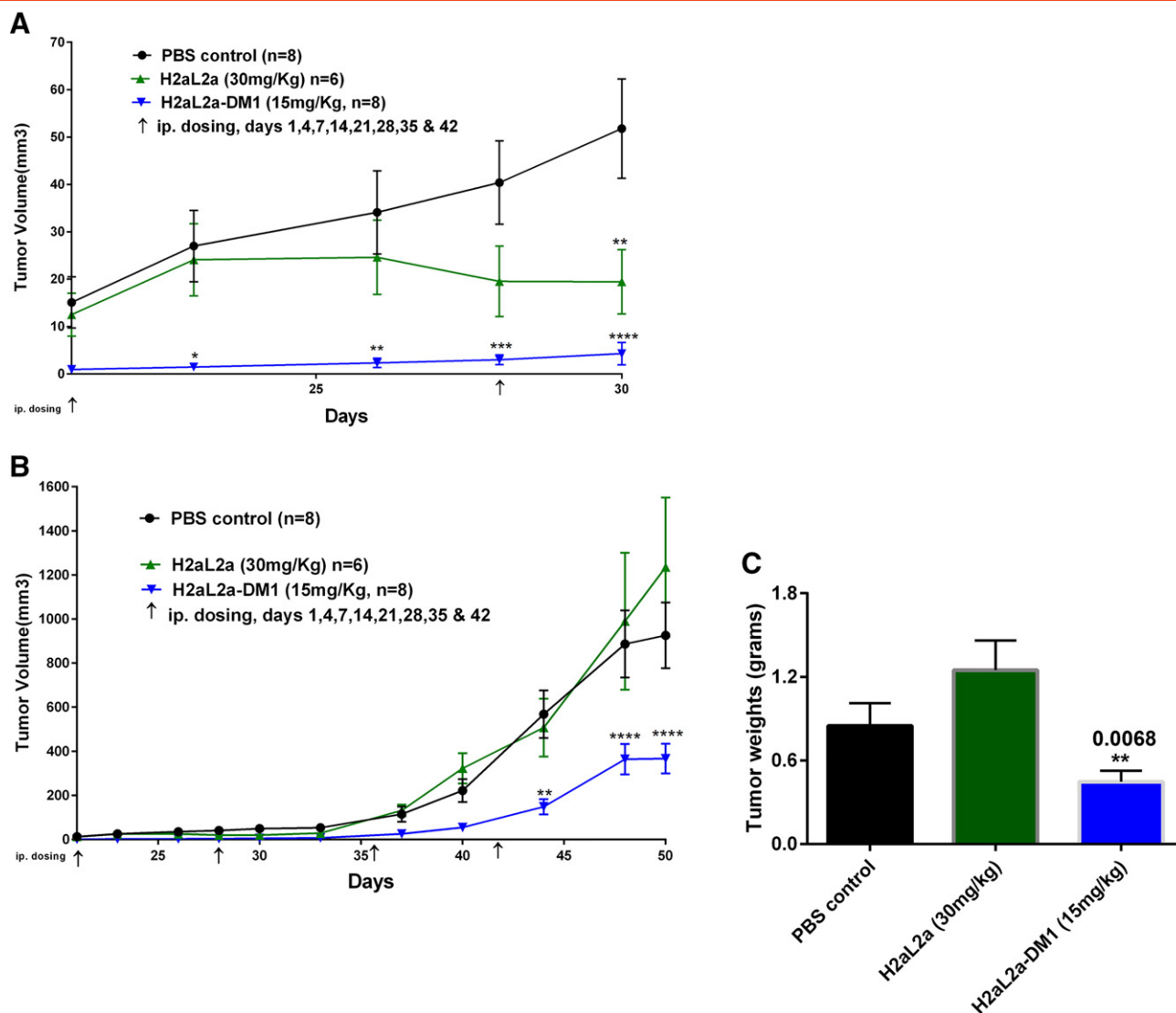


Figure 10. *In vivo* efficacy of H2aL2a and H2aL2a conjugated DM1 in breast tumor model treatment beginning 24 hours after tumor implantation. A) 1×10^7 MDA-MB-231 cells were injected into female SCID mice intra-mammary gland on day 0. Antibody treatment began on day 1 and animals were given i.p. injection of PBS, naked H2aL2a (30 mg/kg), or H2aL2a-DM1 (15 mg/kg). Arrows indicate injection days. n = mice per group. Tumor growth was monitored for 50 days using caliper. A shows the first 30 days of treatment, B is the full 50 day experiment. Two-way ANOVA Analysis of PBS versus H2aL2a-DM1 * $P = .05$, ** $P = .01$, **** $P < .001$. C) Bar graphs representing the mean tumor weights \pm S.E in the control and antibody treatment groups of tumors removed at day 50. * Unpaired t test was used to analyze the PBS control versus H2aL2a-DM1.

Together, the results suggest that hJAA-F11 H2aL2a, both conjugated to DM1 and the naked antibody have potential as adjunct therapy for TNBC, even though this xenograft model was not optimized, since MDA-MB-231 is a low to moderate TF-Ag expresser and the H2aL2a is a lower affinity hJAA-F11 construct than the more recently acquired H3L3 construct. Currently, the ADCs, Kadcyla and Adcetris, have successfully shown efficacy in cancer patients. Adcetris contains an antibody which targets CD-30 that is conjugated to monomethyl auristatin, and is applicable in Hodgkin's lymphoma and systemic anaplastic large cell lymphoma [31]. Kadcyla contains antibody that is conjugated to a microtubulin inhibitor, and is applicable to the 20% of breast cancers that are Her-2 over-expressers [58]. However, whereas Kadcyla is applicable in only about 25% of breast cancer patients, based on preliminary testing, JAA-F11 and our humanized JAA-F11 antibodies should be applicable in up to 80% of breast cancers. Given that TF-Ag is highly expressed on

metastatic breast tumors and plays a major role in the processes associated with tumor metastasis [16–22], the critical new finding that our constructs are internalized by tumor cells makes our humanized antibody an ideal candidate for antibody-drug conjugate therapy specifically for metastatic breast cancers.

Conclusion

In conclusion, this study highlights the therapeutic potential of our hJAA-F11 H2aL2a and H3L3 antibodies. Further development and optimization of these humanized anti-TF-Ag antibodies could lead to their use in direct immunotherapy and use as an antibody-drug conjugate, in conjunction with other approaches for treating breast, lung, and other cancers. Importantly, hJAA-F11 holds great promise, especially for triple-negative breast cancers for which there are no current successful targeted therapies.

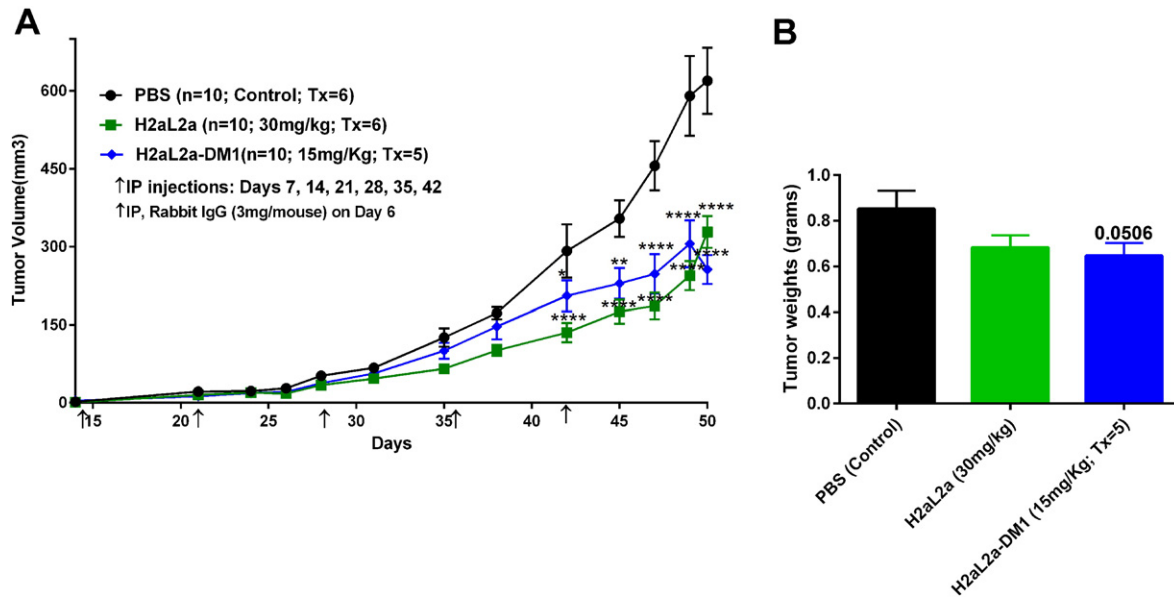


Figure 11. *In vivo* efficacy of H2aL2a and H2aL2a conjugated DM1 in breast tumor model treatment with antibody treatment beginning at day seven after tumor implantation. A) 1×10^7 MDA-MB-231 cells were injected into female SCID mice intra-mammary gland on day 0. Antibody treatment began on day 7 and animals were given i.p. injection of PBS, H2aL2a (30 mg/kg), or H2aL2a-DM1 (15 mg/kg). Mice were injected once a week for 6 weeks. Arrows indicate injection days. $n = 10$ mice per group. Tumor growth was monitored for 50 days. ANOVA Analysis of PBS versus H2aL2a-DM1, PBS versus 30 mg/kg H2aL2a ($*P = .05$, $**P = .01$, $****P < .001$). B) Bar graphs representing the mean tumor weights \pm S.E in the control and antibody treatment groups of tumors removed at day 50. * Unpaired t test was used to analyze the PBS control versus H2aL2a-DM1. Treatment groups were approaching significance when tumor weights were compared.

Competing Interests

KRO owns the company, For-Robin, which has licensed the JAA-F11 and hJAA-F11 antibodies from the University at Buffalo. The University at Buffalo and KRO have the patent for the mouse antibody. KRO does not receive any salary or remuneration from the company at this time or at any time in the past. The University of Buffalo, KRO, JA, JYE and SK have applied for a patent for the humanized antibody. Except where noted there are no other competing interests for any of the authors.

Author Contributions

ST performed the animal experiments, the internalization experiments, the ADCC and the flow experiments, JF worked on all

molecular aspects of this paper, as well as the IC₅₀ experiments, and LK and TC did the original biological experiments; JA, JYE, and SK worked on early molecular aspects of the paper; JA also performed biological experiments, SMM performed the cell culture; FZ, JJ, and DG performed the relative affinity experiments; DG also assisted with the animal experiments; LK and DM performed some internalization experiments. VVG and OVG performed the flow cell experiment; SQ designed and analyzed the flow cytometry; ST, JF, JA, LK, JO, and KRO all prepared the draft of the manuscript. MS, AG, and KG prepared and analyzed the DM-1 conjugate; JO and KRO conceived this study and participated in its design and coordination. All authors read and approved the final manuscript.

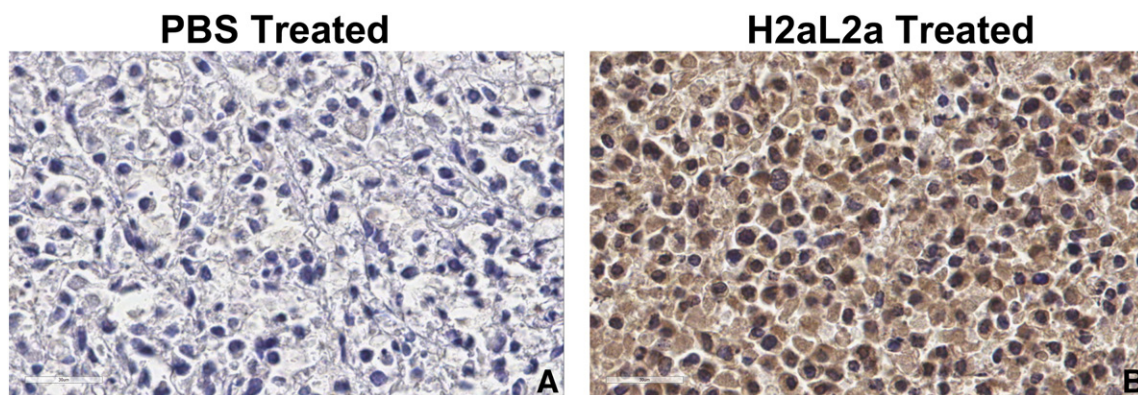


Figure 12. Immunohistochemistry to show tumor localization of H2aL2a after treatment of tumor bearing mice. The tumors from mice in the treatment study shown in Figure 11, injected with either PBS (A) or H2aL2a (B) were fixed, embedded and sectioned and stained using immunohistochemistry for the presence of human IgG in the tumor using anti-human secondary antibody. This shows the presence of H2aL2a binding to the tumor, while PBS indicates minimal background staining alone.

Acknowledgements

The authors would like to acknowledge NIH STTR grants 1 R41 CA176951-01 (KRO) and 2 R42 CA176951-02A1 (KRO) Clinical Translation of an Anti-Metastatic Antibody for Breast Cancer Therapy and Clinical Translation of an Anti-Metastatic Antibody for Breast Cancer Therapy and UB CAT 13-14 For-Robin: UB CAT: Humanization of JAA-F11 for Cancer Immunotherapy Supplement. We would also like to thank the Malaysian government for the support of J. Abdullah. The authors would like to acknowledge The Consortium for Functional Glycomics funded by the NIGMS GM98791 and the National Center for Functional Glycomics funded by P41GM103694 for services provided by the Glycan Array Synthesis Core (The Scripps Research Institute, La Jolla, CA) that produced the mammalian glycan microarray and Dave Smith and Jamie Heimbürg-Molinaro of the Protein-Glycan Interaction Core (Emory University School of Medicine, Atlanta, GA), who assisted with analysis of samples on the array. The authors would also like to acknowledge Andrew Gulick for his modeling analysis of the humanized constructs. This research was also supported in part by the Award #1101BX000609 from the Biomedical Laboratory Research & Development Service of the VA Office of Research and Development (VVG) and the National Cancer Institute of the National Institutes of Health Award #R01CA160461 (VVG)

Appendix A. Supplementary Data

Supplementary data to this article can be found online at <http://dx.doi.org/10.1016/j.neo.2017.07.001>.

References

- Springer GF (1984). T and Tn, general carcinoma autoantigens. *Science* **224**(4654), 1198–1206.
- Springer GF, Murthy MS, Desai PR, and Scanlon EF (1980). Breast cancer patient's cell-mediated immune response to Thomsen-Friedenreich (T) antigen. *Cancer* **45**, 2949–2954.
- Wolf M, Ludwig A, Fritz P, and Schumacher K (1988). Increased expression of Thomsen-Friedenreich antigens during tumor progression in breast cancer patients. *Tumor Biol* **9**(4), 190–194.
- Takanami I (1999). Expression of Thomsen-Friedenreich antigen as a marker of poor prognosis in pulmonary adenocarcinoma. *Oncol Rep* **6**(2), 341–345.
- Cao Y, Karsten UR, Liebrich W, Haensch W, Springer GF, and Schlag PM (1995). Expression of thomsen-friedenreich-related antigens in primary and metastatic colorectal carcinomas. A reevaluation. *Cancer* **76**(10), 1700–1708.
- Ohaka HSH, Yokoyama M, Ochi K, Takeuchi M, and Utsumi S (1985). Thomsen-Friedenreich antigen in bladder tumors as detected by specific antibody: a possible marker of recurrence. *Urol Res* **13**(2), 47–50.
- Ghazizadeh M, Oguro T, Sasaki Y, Aihara K, Araki T, and Springer GF (1990). Immunohistochemical and ultrastructural localization of T antigen in ovarian tumors. *Am J Clin Pathol* **93**(3), 315–321.
- Janssen T, Petein M, Van Velthoven R, van Leer P, Fourmarier M, Vanegas J-P, Danguy A, Schulman C, Pasteels J-L, and Kiss R (1996). Differential histochemical peanut agglutinin stain in benign and malignant human prostate tumors: relationship with prostatic specific antigen immunostain and nuclear DNA content. *Hum Pathol* **27**(12), 1341–1347.
- Moriyama H, Nakano H, Igawa M, and Nihira H (1987). T Antigen Expression in Benign Hyperplasia and Adenocarcinoma of the Prostate (With 1 color plate). *Urol Int* **42**(2), 120–123.
- Chung YS, Yamashita Y, Kato Y, Nakata B, Sawada T, and Sowa M (1996). Prognostic significance of T antigen expression in patients with gastric carcinoma. *Cancer* **77**(9), 1768–1773.
- Cao Y, Merling A, Karsten U, Goletz Steffen, Punzel Michael, Kraft Regine, Butschak Günter, and Schwartz-Albiez Reinhard (2008). Expression of CD175 (Tn), CD175s (sialosyl-Tn) and CD176 (Thomsen-Friedenreich antigen) on malignant human hematopoietic cells. *Int J Cancer* **123**(1), 89–99.
- Aller CT, Kucuk Omer, Springer Georg F, and Gilman-Sachs Alice (1996). Flow cytometric analysis of T and Tn epitopes on chronic lymphocytic leukemia cells. *Am J Hematol* **52**(1), 29–38.
- Almogren A, Abdullah Julia, Ghapure Kshipra, Ferguson Kimiko, Glinsky Vladislav V, and Rittenhouse-Olson Kate (2012). Anti-Thomsen-Friedenreich-Ag (anti-TF-Ag) potential for cancer therapy. *Front Biosci (Schol Ed)* **4**, 840–863.
- Cazet A, Julien Sylvain, Bobowski Marie, Burchell Joy, and Delannoy Philippe (2010). Tumor-associated carbohydrate antigens in breast cancer. *Breast Cancer Res* **12**(3), 204–217.
- Yu L-G (2007). The oncofetal Thomsen-Friedenreich carbohydrate antigen in cancer progression. *Glycoconj J* **24**(8), 411–420.
- Heimbürg J, Yan J, Morey S, Glinskii OV, Huxley VH, Wild L, Klick R, Roy R, Glinsky VV, and Rittenhouse-Olson K (2006). Inhibition of Spontaneous Breast Cancer Metastasis by Anti-Thomsen-Friedenreich Antigen Monoclonal Antibody JAA-F11. *Neoplasia* **8**(11), 939–948.
- Gassmann P, Kang M-L, Mees ST, and Haier J (2010). *In vivo* tumor cell adhesion in the pulmonary microvasculature is exclusively mediated by tumor cell-endothelial cell interaction. *BMC Cancer* **10**(1), 177–188.
- Glinsky VV, Glinsky GV, Rittenhouse-Olson K, Huflejt ME, Glinskii OV, Deutscher SL, and Quinn TP (2001). The role of Thomsen-Friedenreich antigen in adhesion of human breast and prostate cancer cells to the endothelium. *Cancer Res* **61**(12), 4851–4857.
- Glinsky VV, Huflejt ME, Glinsky GV, Deutscher SL, and Quinn TP (2000). Effects of Thomsen-Friedenreich antigen-specific peptide P-30 on β -galactoside-mediated homotypic aggregation and adhesion to the endothelium of MDA-MB-435 human breast carcinoma cells. *Cancer Res* **60**(10), 2584–2588.
- Glinsky VV, Glinsky GV, Glinskii OV, Huxley VH, Turk JR, Mossine VV, Deutscher SL, Pienta KJ, and Quinn TP (2003). Intravascular metastatic cancer cell homotypic aggregation at the sites of primary attachment to the endothelium. *Cancer Res* **63**(13), 3805–3811.
- Yu L-G, Andrews N, Zhao Q, McKean D, Williams JF, Connor LJ, Gerasimenko OV, Hilken J, Hirabayashi J, and Kasai K (2007). Galectin-3 interaction with Thomsen-Friedenreich disaccharide on cancer-associated MUC1 causes increased cancer cell endothelial adhesion. *J Biol Chem* **282**(1), 773–781.
- Zhao Q, Barclay M, Hilken J, Guo X, Barrow H, Rhodes JM, and Yu L-G (2010). Research interaction between circulating galectin-3 and cancer-associated MUC1 enhances tumour cell homotypic aggregation and prevents anoikis. *Mol Cancer* **9**, 154–166.
- Glinskii OV, Li F, Wilson LS, Barnes S, Rittenhouse-Olson K, Barchi Jr JJ, Pienta KJ, and Glinsky VV (2014). Endothelial integrin α 3 β 1 stabilizes carbohydrate-mediated tumor/endothelial cell adhesion and induces macromolecular signaling complex formation at the endothelial cell membrane. *Oncotarget* **5**(5), 1382–1389.
- Rittenhouse-Diakun K, Xia Z, Pickhardt D, Morey S, Baek M-G, and ROY R (1998). Development and Characterization of Monoclonal Antibody to T-Antigen:(Gal β 1-3GalNAc- α -O). *Hybridoma* **17**(2), 165–173.
- Shysh AES, Noujaim AA, Suresh MR, and Longenecker BM (1985). *In vivo* localization of radioiodinated peanut lectin in a murine TA3/Ha mammary carcinoma model. *Eur J Nucl Med* **10**(1–2), 68–74.
- Miller GM, Andres ML, and Gridley DS (2003). NK cell depletion results in accelerated tumor growth and attenuates the antitumor effect of total body irradiation. *Int J Oncol* **23**(6), 1585–1592.
- Chaturvedi R, Heimbürg J, Yan J, Koury S, Sajjad M, Abdel-Nabi HH, and Rittenhouse-Olson K (2008). Tumor immunolocalization using 124 I-iodine-labeled JAA-F11 antibody to Thomsen-Friedenreich alpha-linked antigen. *Appl Radiat Isot* **66**(3), 278–287.
- Ferguson K, Yadav A, Morey S, Abdullah J, Hrysenko G, Eng JY, Sajjad M, Koury S, and Rittenhouse-Olson K (2014). Preclinical studies with JAA-F11 anti-Thomsen-Friedenreich monoclonal antibody for human breast cancer. *Future Oncol* **10**(3), 385–399.
- McQuarrie S, MacLean G, Boniface G, Golberg K, and McEwan A (1997). Radioimmunoscintigraphy in patients with breast adenocarcinoma using technetium-99m labelled monoclonal antibody 170H. 82: report of a phase II study. *Eur J Nucl Med* **24**(4), 381–389.
- Lambert JM (2005). Drug-conjugated monoclonal antibodies for the treatment of cancer. *Curr Opin Pharmacol* **5**(5), 543–549.
- Panowski S, Bhakta S, Raab H, Polakis P, and Junutula JR (2014). Site-specific antibody drug conjugates for cancer therapy. *MAbs*: 2014. Taylor & Francis; 2014. p. 34–45.
- Hwang WYK and Foote J (2005). Immunogenicity of engineered antibodies. *Methods* **36**(1), 3–10.

- [33] Presta LG (2008). Molecular engineering and design of therapeutic antibodies. *Curr Opin Immunol* **20**(4), 460–470.
- [34] Schroff RWFK, Beatty SM, Oldham RK, and Morgan Jr AC (1985). Human anti-murine immunoglobulin responses in patients receiving monoclonal antibody therapy. *Cancer Res* **45**, 879–885.
- [35] Morrison SL (2002). Cloning, expression, and modification of antibody V regions. *Curr Protoc Immunol* [2.12. 11-12.12. 17].
- [36] Kabat EA, Te Wu T, Perry HM, Gottesman KS, and Foeller C (1992). Sequences of proteins of immunological interest. DIANE publishing; 1992 .
- [37] Chothia C, Lesk AM, Tramontano A, Levitt M, Smith-Gill SJ, Air G, Sheriff S, Padlan EA, Davies D, and Tulip WR (1989). Conformations of immunoglobulin hypervariable regions. *Nature* **342**(6252), 877–883.
- [38] Tessier MB, Grant OC, Heimburg-Molinaro J, Smith D, Jadey S, Gulick AM, Glushka J, Deutscher SL, Rittenhouse-Olson K, and Woods RJ (2013). Computational screening of the human TF-glycome provides a structural definition for the specificity of anti-tumor antibody JAA-F11. *PLoS One* **8**(1), e54874.
- [39] Gao SH, Huang K, Tu H, and Adler AS (2013). Monoclonal antibody humanness score and its applications. *BMC Biotechnol* **13**, 55–67.
- [40] Blixt O, Head S, Mondala T, Scanlan C, Huflejt ME, Alvarez R, Bryan MC, Fazio F, Calarese D, and Stevens J (2004). Printed covalent glycan array for ligand profiling of diverse glycan binding proteins. *Proc Natl Acad Sci U S A* **101**(49), 17033–17038.
- [41] Glinskii OV, Turk JR, Pienta KJ, Huxley VH, and Glinsky VV (2004). Evidence of porcine and human endothelium activation by cancer-associated carbohydrates expressed on glycoproteins and tumour cells. *J Physiol* **554**(Pt 1), 89–99.
- [42] Singh R and Erickson HK (2009). Chapter 23-Antibody-Cytotoxic Agent Conjugates: Preparation and Characterization. In: Dmitrov A, editor. *Therapeutic Antibodies: Methods and Protocols*, vol. 525; 2009.
- [43] Tessier M, Makeneni S, Rittenhouse-Olson K, Heimburg-Molinaro J, Jadey S, Gulick A, and Woods RJ (2011). Combining computational carbohydrate threading with glycan array data to define the 3D epitope of an antitumor antibody. *Abstr Pap Am Chem Soc* **241**, 83.
- [44] Van Halbeek H, Breg J, Vliegthart JF, Klein A, Lamblin G, and Roussel P (1988). Isolation and structural characterization of low-molecular-mass mono-sialyl oligosaccharides derived from respiratory-mucus glycoproteins of a patient suffering from bronchiectasis. *Eur J Biochem* **177**(2), 443–460.
- [45] Yurewicz E, Matsuura F, and Moghissi K (1987). Structural studies of sialylated oligosaccharides of human midcycle cervical mucin. *J Biol Chem* **262**(10), 4733–4739.
- [46] Amano J, Nishimura R, Mochizuki M, and Kobata A (1988). Comparative study of the mucin-type sugar chains of human chorionic gonadotropin present in the urine of patients with trophoblastic diseases and healthy pregnant women. *J Biol Chem* **263**(3), 1157–1165.
- [47] Glinskii OV, Li F, Wilson LS, Barnes S, Rittenhouse-Olson K, Barchi Jr JJ, Pienta KJ, and Glinsky VV (2014). Endothelial integrin $\alpha\beta 1$ stabilizes carbohydrate-mediated tumor/endothelial cell adhesion and induces macromolecular signaling complex formation at the endothelial cell membrane; 2014 .
- [48] Glinskii OV, Huxley VH, Glinsky GV, Pienta KJ, Raz A, and Glinsky VV (2005). Mechanical entrapment is insufficient and intercellular adhesion is essential for metastatic cell arrest in distant organs. *Neoplasia* **7**(5), 522–527.
- [49] Carney DN, Gazdar AF, Bepler G, Guccion JG, Marangos PJ, Moody TW, Zweig MH, and Minna JD (1985). Establishment and identification of small cell lung cancer cell lines having classic and variant features. *Cancer Res* **45**(6), 2913–2923.
- [50] Lin WM, Karsten U, Goletz S, Cheng RC, and Cao Y (2011). Expression of CD176 (Thomsen-Friedenreich antigen) on lung, breast and liver cancer-initiating cells. *Int J Exp Pathol* **92**(2), 97–105.
- [51] Banks-Schlegel SP, Gazdar AF, and Harris CC (1985). Intermediate filament and cross-linked envelope expression in human lung tumor cell lines. *Cancer Res* **45**(3), 1187–1197.
- [52] Giard DJ, Aaronson SA, Todaro GJ, Arnstein P, Kersey JH, Dosik H, and Parks WP (1973). In vitro cultivation of human tumors: establishment of cell lines derived from a series of solid tumors. *J Natl Cancer Inst* **51**(5), 1417–1423.
- [53] Stein R, Chen S, Grossman W, and Goldenberg DM (1989). Human lung carcinoma monoclonal antibody specific for the Thomsen-Friedenreich antigen. *Cancer Res* **49**(1), 32–37.
- [54] Kurtenkov O, Klaamas K, Mensdorff-Pouilly S, Miljukhina L, Shljapnikova L, and Chuzmarov V (2007). Humoral immune response to MUC1 and to the Thomsen-Friedenreich (TF) glycotope in patients with gastric cancer: relation to survival. *Acta Oncol* **46**(3), 316–323.
- [55] Kurtenkov OKK, Rittenhouse-Olson K, Vahter L, Sergejev B, Miljukhina L, and Shljapnikova L (2005). IgG immune response to tumor-associated carbohydrate antigens (TF, Tn, alphaGal) in patients with breast cancer: impact of neoadjuvant chemotherapy and relation to the survival. *Exp Oncol* **27**, 136–140.
- [56] Smorodin EPOAKO, Sergejev BL, Chuzmarov VI, and Afanasyev VP (2007). The relation of serum anti-(GalNAc beta) and -para-Forsman disaccharide IgG levels to the progression and histological grading of gastrointestinal cancer. *Exp Oncol* **29**, 61–66.
- [57] Cheung NKV, Guo H, Hu J, Tassev DV, and Cheung IY (2012). Humanizing murine IgG3 anti-GD2 antibody m3F8 substantially improves antibody-dependent cell-mediated cytotoxicity while retaining targeting *in vivo*. *Oncimmunology* **1**(4), 477–486.
- [58] Barok M, Joensuu H, and Isola J (2014). Trastuzumab emtansine: mechanisms of action and drug resistance. *Breast Cancer Res* **16**(2), 209–221.